ChemComm

FEATURE ARTICLE

View Article Online
View Journal | View Issue

Cite this: *Chem. Commun.*, 2024, **60**, 4745

Recent advances in nucleic acid signal amplification-based aptasensors for sensing mycotoxins

Dandan Zhang,[a] Ting Luo,[a] Xiangyue Cai,[a] Ning-ning Zhao*[b] and Chun-yang Zhang *[c]

Received 29th February 2024,
Accepted 8th April 2024

DOI: 10.1039/d4cc00982g

rsc.li/chemcomm

Mycotoxin contamination in food products may cause serious health hazards and economic losses. The effective control and accurate detection of mycotoxins have become a global concern. Even though a variety of methods have been developed for mycotoxin detection, most conventional methods suffer from complicated operation procedures, low sensitivity, high cost, and long assay time. Therefore, the development of simple and sensitive methods for mycotoxin assay is highly needed. The introduction of nucleic acid signal amplification technology (NASAT) into aptasensors significantly improves the sensitivity and facilitates the detection of mycotoxins. Herein, we give a comprehensive review of the recent advances in NASAT-based aptasensors for assaying mycotoxins and summarize the principles, features, and applications of NASAT-based aptasensors. Moreover, we highlight the challenges and prospects in the field, including the simultaneous detection of multiple mycotoxins and the development of portable devices for field detection.

1. Introduction

Food safety has attracted global attention. Food contamination affects the multistep process of the food supply chain from farms to dining tables, and it may originate from agricultural practices, the storage and transportation steps of raw agricultural commodities, industrial food processing, and the storage of foods. The presence of mycotoxins in foodstuff is a most conspicuous and serious concern.[1] Approximately 25% of the world's foods are tainted with mycotoxins every year, and their presence in food affects its quality and safety and may cause serious economic losses and safety risks.[2,3]

Mycotoxins are secondary metabolites of fungal species (*e.g.*, *Aspergillus*, *Penicillium*, *Alternaria*, *Fusarium, Claviceps, and Stachybotrys* species).[4] Due to their teratogenic, mutagenic, carcinogenic, immunosuppressive, and endocrine-disrupting

[a] *College of Materials and Chemistry & Chemical Engineering, Chengdu University of Technology, Chengdu 610059, Sichuan, China*
[b] *College of Chemistry, Chemical Engineering and Materials Science, Shandong Normal University, Jinan 250014, China. E-mail: zhaoningning1997@qq.com*
[c] *School of Chemistry and Chemical Engineering, Southeast University, Nanjing, 211189, China. E-mail: zhangcy@seu.edu.cn*

Dandan Zhang

Dandan Zhang obtained her PhD from Shandong Normal University in 2020. Subsequently, she joined Chengdu University of Technology as a researcher. Her research interest focuses on bioanalytical chemistry, detection, and the control of foodborne contaminants, and on-site food safety detection.

Ting Luo

Ting Luo obtained her BS degree from North Minzu University in 2023. She is currently a master's student under the supervision of Dr Dandan Zhang at Chengdu University of Technology. Her research focuses on the development of functional MOF and COF-based aptasensors for the detection of mycotoxins.

effects, low concentrations of mycotoxins can cause chronic toxicity to humans and other animals through the food chain.[5–9] Most mycotoxins have unique chemical and thermal stability, making them difficult to remove during conventional food processing and disinfection.[2,10] To date, about 400 different mycotoxins have been identified, but only few species are the concerns of food safety. Based on the carcinogenic risk of mycotoxins to human health, International Agency for Research on Cancer (IARC) classifies them into different categories, such as aflatoxins (AFs), zearalenone (ZEN), T2/HT2, deoxynivalenol (DON), patulin (PAT), and ochratoxin A (OTA).[4,6,8,9,11–13] Among them, aflatoxin B1 (AFB1) is one of the most toxic and ubiquitous potential carcinogens, and it is classified into Group 1A. AFB1 may cause lung cancer, hepatocellular cancer, gallbladder cancer, and colon cancer in humans. Approximately 28.2% of liver cancers are induced by AFB1.[14,15] OTA and fumonisin are possibly carcinogenic to humans and are classified into Group 2B.[16–19] Table 1 lists the chemical structures of major mycotoxins and the affected food commodities as well as their toxic effects on humans and animals. The European Union, the Food and Drug Administration of the USA, and the Chinese Pharmacopoeia Commission have established regulatory guidelines and maximum residue levels (MRLs) for the majority of toxic mycotoxins prevalent in certain commodities to protect human health (Table 1). To meet these strict requirements, the development of sensitive and reliable analytical methods to detect mycotoxins in diverse matrices at trace levels is extremely urgent.[9]

Chromatography is the earliest and most conventional method for mycotoxin assay,[20] including high-performance liquid chromatography (HPLC), thin layer chromatography (TLC), gas chromatography (GC), liquid chromatography-tandem mass spectrometry (LC-MS), HPLC coupled with mass spectroscopy (HPLCMS).[21–25] Despite the high sensitivity and accuracy of these methods, they often require expensive instruments, professional operators, and cumbersome pre-treatment steps.[26] Antibody-based immunoassays (*e.g.*, enzyme-linked immunosorbent assay (ELISA), lateral flow immunoassays (LFIA), and colloidal gold immune chromate graphic assay (GICA))[27–29] can achieve the rapid and accurate quantification of mycotoxin.[30,31] However, these methods suffer from semi-quantification, false positive results, poor repeatability, and long reaction times.[32] In addition, the antibodies used in these methods suffer from complex preparation processes, high costs, poor stability, and low immunogenicity, which limits their wider application.

Aptamers are single-stranded oligonucleotides (DNA or RNA) that mimic monoclonal antibodies and are screened through a selection process, namely the systematic evolution of ligands by exponential enrichment (SELEX).[33] Compared with antibodies, aptamers have distinct advantages of high binding affinity, good specificity, excellent stability, easy modification, low cost, little batch-to-batch differences, and a wide range of targets.[33–36] As a new kind of highly selective biological recognition element, aptamers have been widely used in the construction of biosensors for mycotoxin assays.[37–46] In terms of sensor components, aptasensors usually include an

Xiangyue Cai

Xiangyue Cai obtained her BS degree from Chengdu Normal University in 2021. She is a master's student under the guidance of Dr Dandan Zhang at Chengdu University of Technology. Her research interest focuses on the development of aptasensors for the detection of mycotoxins in food products.

Ning-ning Zhao

Ning-ning Zhao obtained her BS degree from Xinjiang Normal University in 2019. Currently, she is a research assistant at Shandong Normal University. Her research focuses on bioanalytical chemistry and single-molecule detection.

Chun-yang Zhang

Chun-yang Zhang obtained his PhD degree from Peking University, China, in 1999. From 1999–2008, he worked at Tsinghua University, China, Emory University, USA, Johns Hopkins University, USA, and the City University of New York, USA. In 2009, he joined in the Shenzhen Institute of Advanced Technology, Chinese Academy of Sciences, China. From 2015–2023, he worked as the Dean of the College of Chemistry, Chemical Engineering, and Material Science at Shandong Normal University, China. In 2023, he joined Southeast University, China. He is the recipient of the China National Fund for Distinguished Young Scientists.

Table 1 A summary of major mycotoxins and their characteristics, as well as the maximum permitted levels of mycotoxins in foods according to regulations by China, the European Union (EU)[a], and the United States (U.S.)

Mycotoxins	Structure	Molar mass ($g\ mol^{-1}$)	Commodities affected	Toxic effects	Country	Maximum permitted lever ($\mu g\ kg^{-1}$)	Ref.
AFB1	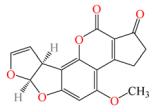	312.27	Grains such as maize, rice, wheat, milk and milk products, *etc.*	Carcinogenic, teratogenic, mutagenic, immunosuppressive	China EU U.S.	5–20(0.5)[c] 2–12(0.1)[c] 20	55
OTA	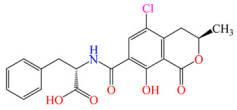	224.19	Cereals, wine, coffee, cocoa, beans, dried fruits, nuts, spices, cheese, *etc.*	Nephrotoxic, hepatotoxic, neurotoxic, teratogenic, immunotoxic	China EU U.S.	2–10 2–80(0.5)[c] Not set	56
DON	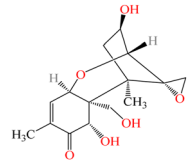	296.32	Cereals, cereal products	Diarrhea, vomiting, anorexia, immune dysregulation	China EU U.S.	1000 500–1750, (200)[c] 1000	57
ZEN	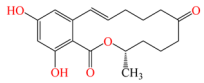	318.36	Cereals, cereal products, maize, rice, beer, *etc.*	Hyperoestrogenic, hepatotoxic, haematotoxic, immunotoxic, genotoxic	China EU U.S.	60 50–400(20)[c] Not set	58
AFM1	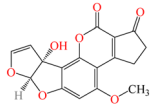	584.87	Milk, dairy	Carcinogenic, cytotoxic, hepatotoxic	China EU U.S.	0.5 0.05(0.025)[c] 0.5	55
T-2	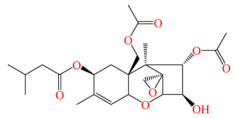	466.52	Wheat, rye, maize, soybeans	Growth retardation, myelotoxic, hemotoxic, necrotic lesions on contact sites	China EU U.S.	Not set In preparation[b] 2000–4000	59
PAT	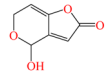	154.12	Fruits and vegetables	Nausea, vomiting, and other gastrointestinal symptoms, kidney damage	China EU U.S.	50 25–50, (10)[c] 50	60

[a] Regulations (EC) No. 2002/32/EC, 1881/2006, 2021/1399. [b] 2013/165/EU: Commission. Recommendation. [c] The number in brackets refers to infant food and young children.

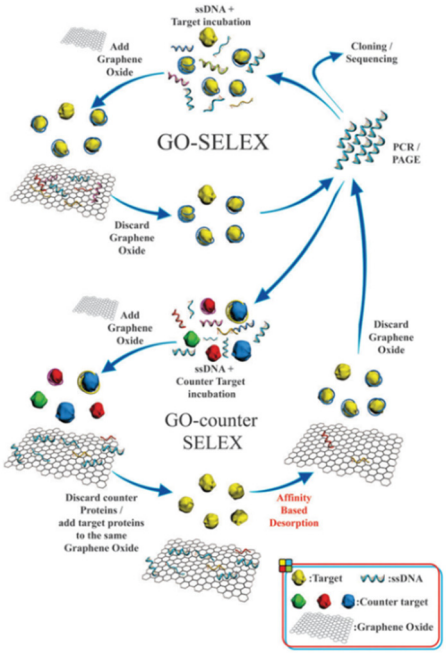

Fig. 1 Schematic illustration of the steps involved in the GO-SELEX procedure of aptamer identification.[54]

aptamer-based target recognizer and a signal transducer. Because mycotoxins are usually measured in ppb (parts per billion), the achievement of a detection limit in nanograms has become a great challenge.[47] Therefore, the development of nucleic acid signal amplification-based aptasensors is crucial for the achievement of sensitive detection of mycotoxins in real samples.

2. Aptamer sequences used in mycotoxin detection

The capability of aptamers to specifically identify target molecules is critical to improving the selectivity and sensitivity of aptasensors, and the integration of SELEX with graphene oxide (GO) has been applied to screen mycotoxin aptamers with high affinity.[48–53] The non-specific adsorption of the single-stranded DNA (ssDNA) random library on GO is the basis for separating unbound DNA in the GO-SELEX process.[54] The individual steps involved in one GO-SELEX and GO-counter SELEX round are illustrated in Fig. 1. In the first step of affinity selection, a preincubated mixture of the random ssDNA library and the target is incubated with GO solution. Subsequently, the free unbound ssDNAs are adsorbed on GO and then removed by centrifugation. The supernatant with ssDNAs bound to the target is then recovered, amplified, and purified for a further GO-counter SELEX process to eliminate the false positive binding of aptamers. In the GO-counter SELEX process, affinity-based desorption is triggered by incubating GO with the target to restore the adsorbed ssDNA on GO. Eventually, the recovered ssDNAs are purified, cloned, and sequenced to obtain the final hit aptamers. A series of mycotoxin aptamers have been successfully screened (Table 2),[61–68] including AFB1, OTA, Aflatoxin M1 (AFM1), and ZEN. Notably, the aptamers for other mycotoxins are rarely reported, except for the aptamers of the PAT and T-2 toxins. Due to the complexity of food substrates and the trace levels of mycotoxins in the substrates, the sensitive detection of mycotoxins remains a challenge.

3. Nucleic acid signal amplification techniques

To achieve the sensitive detection of trace mycotoxins in complex matrices, signal amplification strategies have been introduced into the construction of aptasensors.[69,70] The nucleic acid signal amplification technique (NASAT) takes advantage of various enzymes, nucleases, and deoxyribozyme (DNAzyme) to amplify the signal,[71,72] and the integration of NASAT with aptamers can greatly improve the sensitivity of the mycotoxin assay.[66–80] NASAT is divided into enzyme-assisted nucleic acid amplification and enzyme-free amplification. Enzyme-assisted nucleic acid amplification includes polymerase chain reaction (PCR), rolling circle amplification (RCA), strand displacement amplification (SDA), nuclease-assisted amplification, and CRISPR/Cas system-related amplification. Enzyme-free amplification includes catalytic hairpin assembly (CHA), hybridization chain reaction (HCR), DNA walker, DNA tweezer, and DNAzyme.

Table 2 Sequences of mycotoxin aptamers (from 5′ to 3′)

Target	Aptamer sequence (from 5′ to 3′)	Kd (nM)	Ref.
OTA	GATCGGGTGTGGGTGGCGTAAAGGGAGCATCGGACA	0.36	52
	AGCCTCGTCTGTTCTCCCGGCAGTGTGGGCGAATCTATGCGTACCGTTCGATATCGTGGGGAAGACAAGCAGACGT	290 ± 150	49
	GGCAGTGTGGGCGAATCTATGCGTACCGTTCGATATCGTG	406 ± 166	94
AFB1	GTTGGGCACGTGTTGTCTCTCTGTGTCTCGTGCCCTTCGCTAGGCCCACA	0.59 ± 0.33	95
	AGCAGCACAGAGGTCAGATGGTGCTATCATGCGCTCAATGGGAGACTTTAGCTGCCCCCACCTATGCGTGCTACCGTGAA	11.29 ± 1.27	96
	CTCGTCTCGTTCTCTCAGTCTGGTTAGCACGGGACCCAGGCTATTGGCAACTTCTAGTCCGACACGAAGAAGAAGGAGGA	48.29 ± 9.45	97
AFM1	GTTGGGCACGTGTTGTCTCTCTGTGTCTCGTGCCCTTCGCTAGGCCCACA	10	98
	ATCCGTCACACCTGCTCTGACGCTGGGGTCGACCCGGAGAAATGCATTCCCCTGTGGTGTTGGCTCCCGTAT	35.6 ± 2.9	99
ZEN	TCATCTATCTATGGTACATTACTATCTGTAATGTGATATG	41 ± 5	100
DON	GCATCACTACAGTCATTACGCATCGTAGGGGGGATCGTTAAGGAAGTGCCCGGAGGCGGTATCGTGTGAAGTGCTGTCCC	—	101
T-2	CAGCTCAGAAGCTTGATCCTGTATATCAAGCATCGCGTGTTTACACATGCGAGAGGTGAAGACTCGAAGTCGTGCATCTG	20.8 ± 3.1	48
PAT	GGCCCGCCAACCCGCATCATCTACACTGATATTTTACCTT	21.83 ± 5.022	102

3.1. Enzymatic amplification-based aptasensors

In recent years, enzymatic amplification technology has been widely used for mycotoxin detection. The enzyme-assisted nucleic acid amplification techniques mainly focus on PCR, RCA, SDA, nuclease-assisted strategies, and the CRISPR/Cas system.

3.1.1. Polymerase chain reaction (PCR). PCR is a thermal cycle amplification method that can quickly amplify a large number of DNA copies.[73,74] The PCR amplification-based aptasensors have obvious advantages of high sensitivity, good specificity, fast detection speed, and good accuracy.

Walter *et al.* developed a target-induced dissociation (TID)-based aptamer-assisted real-time PCR assay to detect OTA (Fig. 2A).[75] The OTA aptamers are immobilized on the dT-modified magnetic beads (dT beads, where dT is $d(T)_{25}$). When OTA is present, the aptamer is released from the dT beads as a result of TID, and the magnetic beads are separated with a magnetic stand. The released aptamers are amplified and quantified by qPCR. This assay can sensitively detect OTA with a limit of detection (LOD) of 0.009 ng mL^{-1}. Moreover, the Apta-qPCR can be easily extended to detect other mycotoxins.

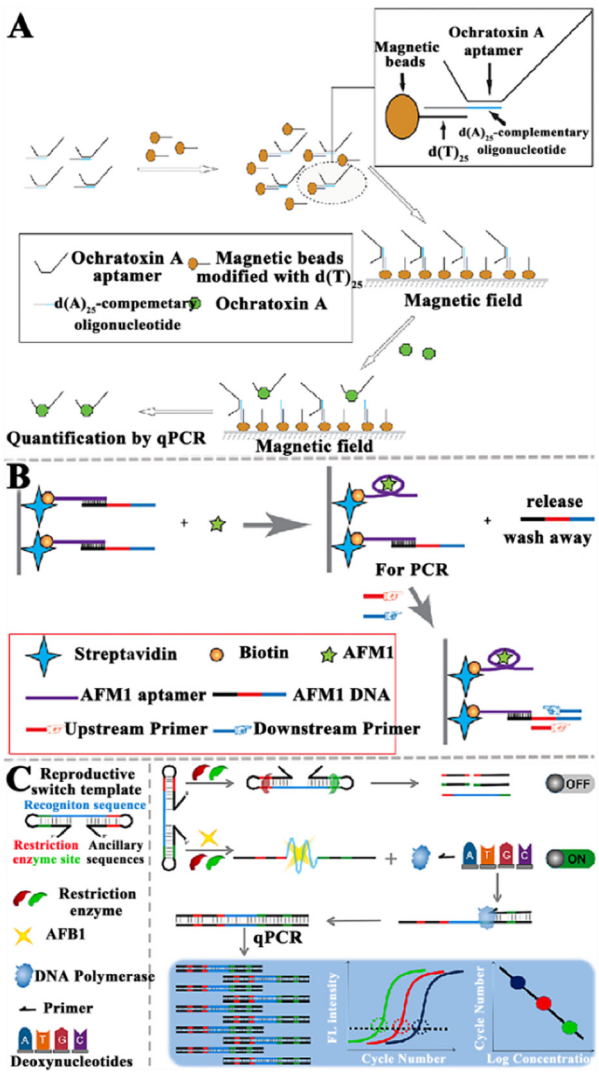

Fig. 2 The construction of aptasensors based on PCR-assisted signal amplification for the mycotoxin assay. (A) The construction of an RT-qPCR-based aptasensor for the OTA assay.[75] (B) The construction of an RT-qPCR-based aptasensor for the AFM1 assay.[76] (C) Construction of a qPCR-based aptasensor for the AFB1 assay.[77]

Wang *et al.* constructed an aptamer-based biosensor to sensitively and selectively detect AFM1 (Fig. 2B).[76] The aptamer is immobilized based on strong interactions between biotin and streptavidin. The presence of AFM1 induces the release of complementary ssDNA due to the formation of an aptamer/AFM1 complex, and then the released ssDNA acts as the template for RT-qPCR amplification. Finally, AFM1 can be quantified according to the linear relationship between the change in PCR amplification signal and the AFM1 level. This aptasensor exhibits high sensitivity with a LOD of 0.03 ng L^{-1}, and it can be applied in the quantitative detection of AFM1 in infant rice cereal and infant milk powder samples. Notably, this approach is potentially useful for food safety analysis, and it can be extended to the detection of a large number of targets.

He *et al.* established a qPCR method-based aptasensor for the sensitive detection of AFB1 (Fig. 2C).[77] When AFB1 is present, the template can be switched from a dumbbell-shaped structure to a linear structure. Due to the restriction, enzymes cannot act on the linear template, and the linear DNA templates are subjected to qPCR for the sensitive quantification of AFB1. This method achieves a LOD of 0.03 pg mL^{-1} and it can be applied for quantification of AFB1 in complex foods (*e.g.*, soy sauce, milk, yellow wine, and peanut butter). This work extends the application of qPCR to non-nucleic acid detection, providing a new approach for the sensitive detection of small-molecule toxicants in foods. Although PCR is the most widely used technology for nucleic acid signal amplification, it still has some shortcomings. For instance, PCR requires thermal cycle amplification instruments and complex amplification procedures, which cannot be implemented at ambient temperature. In addition, some false-positive results and cross-contamination from amplicons often occur in PCR amplification.[78,79]

3.1.2. Rolling circle amplification (RCA). RCA is a simple and efficient enzymatic amplification process that utilizes circular templates, deoxynucleotide triphosphate (dNTP), primers, DNA and RNA polymerases (*e.g.*, Phi29, Bst, and Vent exo-DNA polymerase for DNA, and T7 RNA polymerase for RNA) to produce long single-stranded DNA (ssDNA) and single-stranded RNA (ssRNA).[80,81] Taking advantage of specific template sequences, RCA can generate functional sequences such as DNA aptamers,[82,83] DNAzymes,[84–87] spacer domains[83] and restrict enzyme sites.[88,89] RCA products can also be hybridized with complementary oligonucleotides tethered to functional moieties, such as fluorophores, biotin, antibodies, and nanoparticles, for biometric recognition, sensing, and imaging.[90–93]

Various RCA-based aptasensors have been established for mycotoxin detection. Chen *et al.* developed an electrochemical aptasensor to detect OTA based on RCA-assisted signal amplification (Fig. 3A).[103] In this aptasensor, the RCA primer is

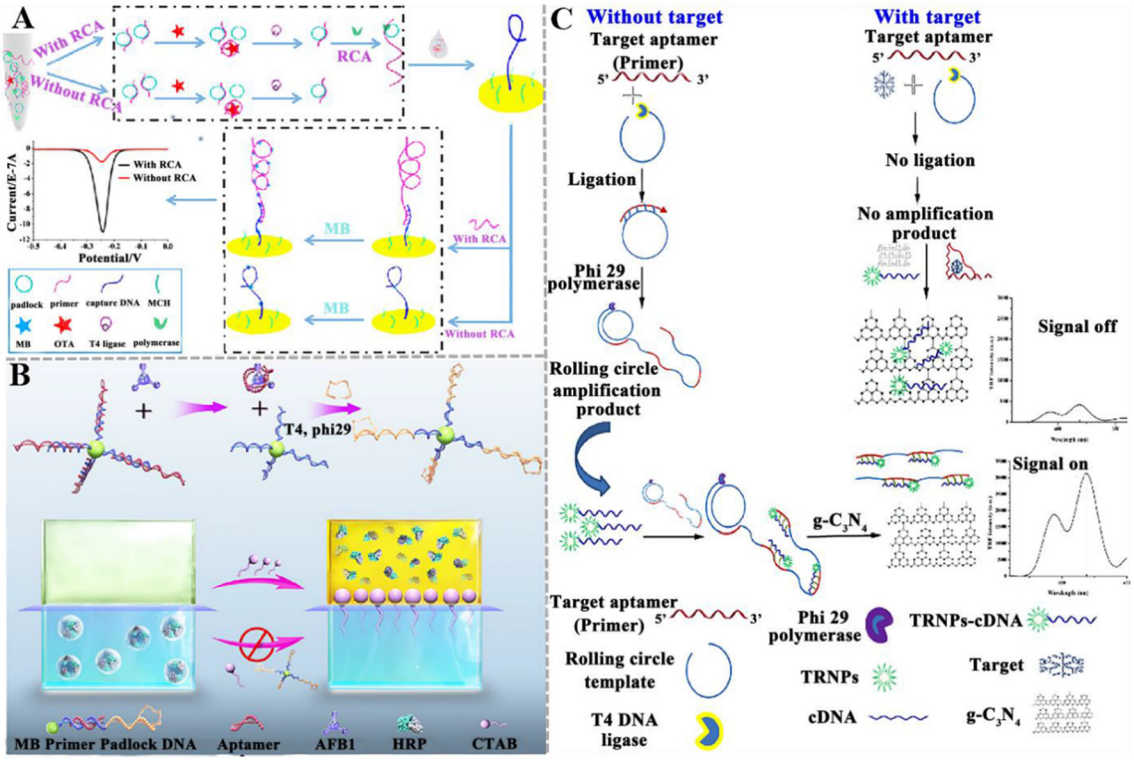

Fig. 3 The construction of aptasensors based on RCA-assisted signal amplification for mycotoxin detection. (A) The construction of an electrochemical aptasensor for the OTA assay based on RCA-assisted signal amplification.[103] (B) The construction of a colorimetric aptasensor for the AFB1 assay based on RCA-assisted signal amplification.[104] (C) The construction of a fluorescent aptasensor for the AFM1 assay based on TRFNPs combined with RCA.[105]

composed of a two-part sequence, including the aptamer sequence of OTA and a partially complementary sequence of the capture probe on the electrode surface. When OTA is present, it preferentially binds with the RCA primer, inducing the disassociation of primer from the padlock. Under these circumstances, RCA cannot be initiated, and the primer cannot be prolonged. As a result, methylene blue (MB) cannot bind to the guanine bases of DNA molecules, inducing a decrease in the electrochemical signal. This aptasensor shows good specificity and high sensitivity with a LOD of 0.065 pg mL^{-1}, and it can accurately measure OTA in wine samples. Hu *et al.* constructed a colorimetric liquid crystal (LC)-based aptasensor for AFB1 detection (Fig. 3B). The microdroplets were formed by introducing the aqueous mixture solution of horseradish peroxidase (HRP) and sodium dodecyl sulfate (SDS) into the LCs, encapsulating HRP in the microdroplets and stabilizing with SDS. Upon the addition of cetyl trimethyl ammonium bromide (CTAB), HRP is ejected from the LCs into the overlaying aqueous solution due to the interfacial charge interaction, and it subsequently catalyses the colorless 3,3′,5,5′-tetramethylbenzidine (TMB) into yellow products. In the presence of AFB1, the binding of the aptamer with AFB1 induces the dissociation of the aptamer/primer duplex decorated on MBs, initiating the RCA reaction to generate long-chain ssDNAs on magnetic beads (MBs).[104] Due to the complete capture of CTAB by the amplified ssDNA, the release of HRP into the aqueous solution is prevented and no color change is observed. This assay can sensitively detect AFB1 with a LOD of 0.014 pg mL^{-1}, and it can measure AFB1 in rice and peanut oil. Wang and co-workers reported a competitive ''signal-off'' fluorescent aptasensor for AFM1 detection based on the combination of time-resolved fluorescent nanoparticles (TRFNPs) with RCA (Fig. 3C).[105] In this assay, the AFM1 aptamer serves as an RCA primer for DNA amplification. In the absence of AFM1, the rolling circle template (RCT) is complementary to the aptamer and ligated by T4 DNA ligase to generate the RCA template. Upon the addition of phi29 DNA polymerase, the RCA reaction is initiated to generate long ssDNA roll-loop amplification products (RCAPs) containing multiple AFM1 aptamers. Since TRFNPs-cDNA complements the aptamer sequence to form an RCAP/TRFNPs-cDNA duplex that cannot be adsorbed on graphitic carbon nitride (g-C_3N_4) nanosheets, the fluorescence of TRFNPs is not quenched. When AFM1 is present, the aptamer recognizes the target AFM1 to form an aptamer-target complex, and there is neither the occurrence of RCA nor the formation of the duplex. The free signal probe TRFNPs-cDNA adsorbs on the g-C3N4, resulting in the quenching of fluorescence. The assay exhibited a LOD of 0.0194 pg mL^{-1} and a recovery ratio of 92–99.8%.

Although a series of RCA-based aptasensors have been developed for the sensitive detection of mycotoxins, there are still some limitations. For example, the efficiency of RCA amplification is easily affected by the lock-probe hybridization and the efficiency of the probe-template connection and

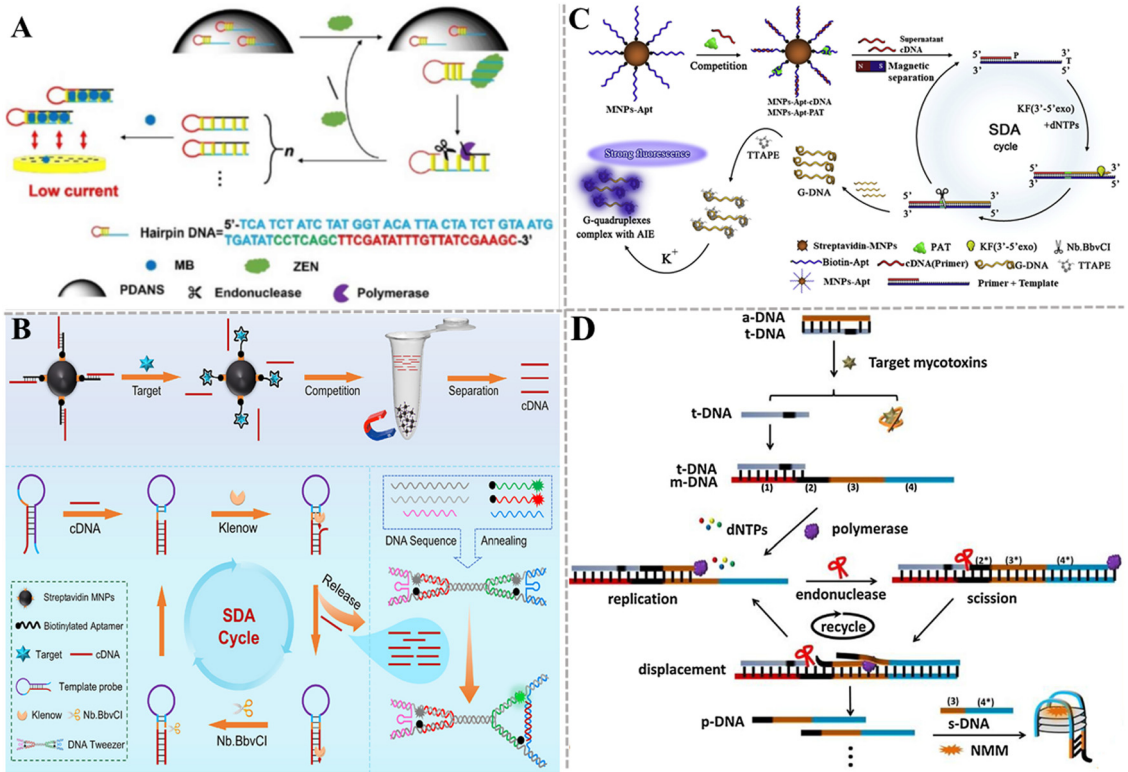

Fig. 4 The construction of aptasensors based on SDA for mycotoxin detection. (A) The construction of an electrochemical aptasensor for the ZEN assay based on target-induced SDA.[110] (B) The construction of a fluorescent aptasensor based on programmable DNA tweezers and SDA for the detection of AFB1 and ZEN.[111] (C) The construction of an aptasensor based on SDA and DNA G-quadruplex for the PAT assay.[112] (D) The construction of a label-free aptasensor for AFM1 and OTA detection.[113]

single-stranded template restriction. When the RCA template is linear DNA, the circularization of the RCA template requires additional enzymes and procedures, increasing the cost and operational complexity.

3.1.3. Strand displacement amplification (SDA). SDA is an isothermal and simple method for the *in vitro* amplification of DNA.[106] The continuous cycle of polymerization, nicking, and displacement of SDA can lead to exponential amplification and produce approximately 10^7 target fragments within 2 h at 37 °C.[70,107–109] The combination of SDA with aptamer-based aptasensors has been applied in mycotoxin detection.

Xu *et al.* developed a target-induced SDA electrochemical aptasensor for the detection of ZEN (Fig. 4A).[110] When ZEN is present, it binds with the aptamer section of multifunctional hairpin DNA anchored on the surface of polydopamine nanospheres (PDANSs, which act as a carrier), leading to the release of multifunctional hairpin DNAs into the solution. Then, the SDA reaction is initiated with the assistance of polymerase and endonuclease, producing abundant negatively charged dsDNA. Methylene blue (MB) molecules are embedded into the dsDNA grooves to obtain the complex with a negative charge. These complexes are electrostatically repelled on the ITO electrode with a negative charge, inducing a decrease in current intensity. This electrochemical aptasensor can detect ZEN in corn flour with a LOD of 0.18 pg mL^{-1}. This electrochemical aptasensor can be used to monitor other mycotoxins by simply changing the corresponding aptamer. Gao *et al.* developed a fluorescent aptasensor based on a programmable DNA tweezer and SDA for the detection of AFB1 and ZEN (Fig. 4B).[111] They synthesized the aptamer-functionalized magnetic nanoparticles (MNPs). When target AFB1 or ZEN is present, it binds with the aptamer, liberating the cDNA after magnetic separation. The hairpin-structure DNA is complementarily paired with the cDNA, inducing the opening of the initial hairpin structure to form another hairpin structure, initiating the SDA reaction with the aid of KF polymerase and Nb.BbvCI to achieve exponential amplification of cDNA. Subsequently, the amplification product cDNAs are added to the DNA tweezers system to generate a distinct signal output. This strategy shows high sensitivity with a LOD of 0.933 pg mL^{-1} for AFB1 and 1.07 pg mL^{-1} for ZEN. Moreover, this method can be easily adapted to detect other analytes by just substituting the aptamer and cDNA.

Liu *et al.* took advantage of SDA, DNA G-quadruplex, and aggregation-induced emission (AIE) to develop an aptasensor for the sensitive and rapid detection of PAT (Fig. 4C).[112] The aptamer is modified on magnetic beads *via* biotin–streptavidin interaction. After the cDNA and PAT competitively bind with aptamers, the cDNA is separated by magnetic separation and serves as a primer of SDA to generate plenty of G-rich ssDNAs. The G-rich ssDNA can form the G-quadruplex that can be stained by TTAPE dye to produce a fluorescence signal in the presence of K^+, and the aggregation of more TTAPEs generates

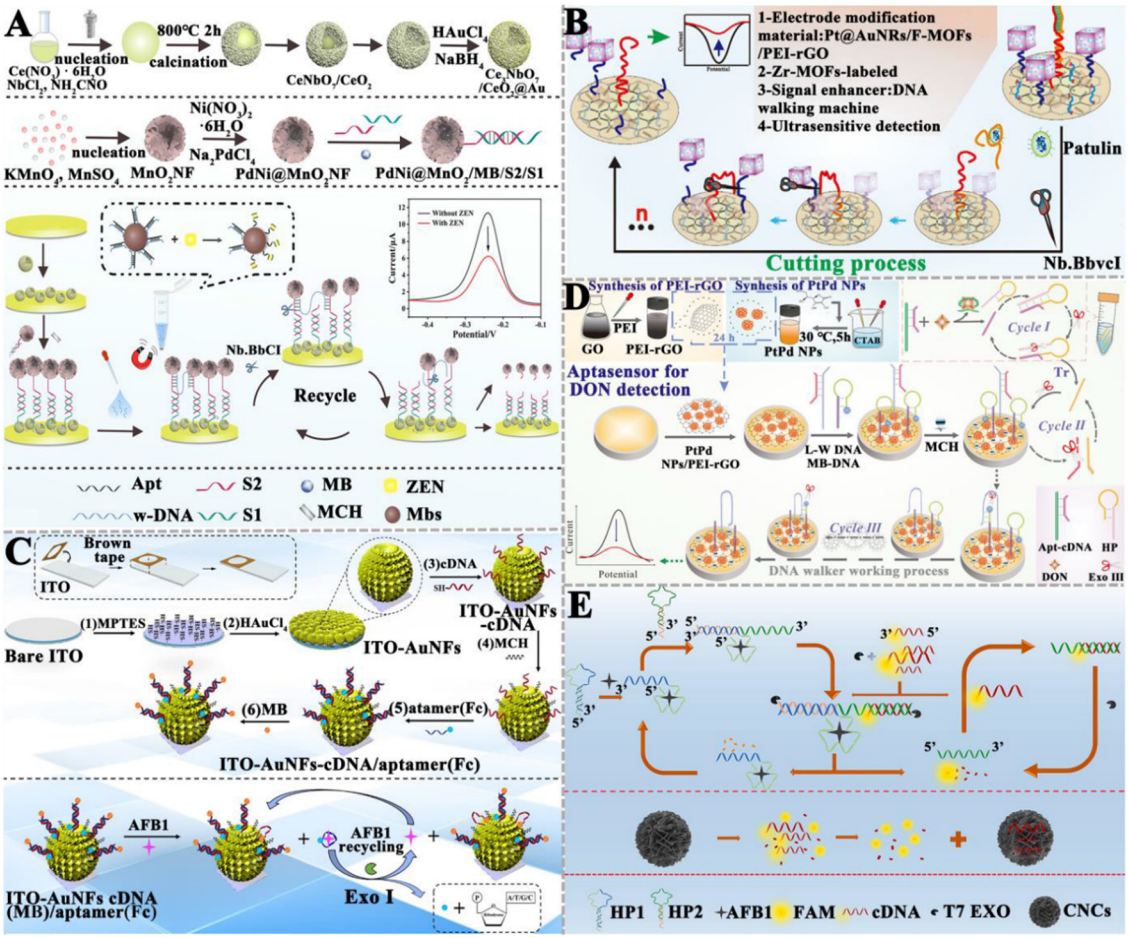

Fig. 5 The construction of nuclease-based aptasensors for mycotoxin detection. (A) The construction of an electrochemical aptasensor based on the Nb.BbvCI-triggered and bipedal DNA walker amplification for the ZEN assay.[115] (B) The construction of an electrochemical aptasensor based on the Nb.BbvCI-powered DNA walking for the PAT assay.[116] (C) The construction of an electrochemical aptasensor based on EXO I-assisted target recycling amplification for the AFB1 assay.[117] (D) The construction of an electrochemical aptasensor based on Exo III-powered WDNA for the DON assay.[118] (E) The construction of a fluorescent aptasensor based on the T7 Exo double recycling amplification for the AFB1 assay.[119]

a stronger fluorescence signal. This assay exhibits good specificity and high sensitivity with a LOD of 0.042 pg mL^{-1}. Gao *et al.* presented a label-free method based on SDA and a G-quadruplex-specific fluorescence probe for AFM1 and OTA detection (Fig. 4D).[113] In this assay, the aptamer (a-DNA) hybridizes partly with a DNA strand (t-DNA). The presence of target mycotoxin triggers SDA to generate plenty of DNA (p-DNA) products with the assistance of polymerase and nicking endonuclease. Subsequently, p-DNA and s-DNA form a G-quadruplex that can act as the signal-transducing element to enhance the fluorescence of *N*-methyl mesoporphyrin IX (NMM). This strategy can distinguish different target mycotoxins using the corresponding aptamers. The LOD is 17.79 ng kg^{-1} for AFM1 and 18.98 ng kg^{-1} for OTA.

3.1.4. Nuclease-assisted amplification. Superior to polymerase-catalyzed signal amplification that requires multiple sensing elements (*e.g.*, dNTPs, rNTPs, primer, and template), nucleases can induce efficient signal amplification through a simple cyclic cleavage process, avoiding high background signals derived from nonspecific polymerization.[72] The nuclease-based amplification has many distinct advantages of facile design, simple operation, rapid reaction, and easy development.[114] Various nucleases including endonucleases and exonucleases (*e.g.*, Exo I, Exo III, and T7 Exo) have been exploited for mycotoxin detection. The Liu group constructed an electrochemical aptasensor based on the Nb.BbvCI-triggered bipedal DNA walker for the ultrasensitive detection of ZEN (Fig. 5A).[115] The aptasensor used Ce_3NbO_7/CeO_2 @Au hollow nanospheres as the electrode modification material and PdNi@MnO_2/MB as the signal label. The duplex structure formed by ZEN aptamers and w-DNA was anchored to the carboxylated MBs. In the presence of ZEN, it specifically binds to the aptamer, resulting in the release of the bipedal DNA walker (w-DNA). Subsequently, the w-DNA is cast on the electrode, initiating cyclic signal amplification. The w-DNA can spontaneously walk on S2 in the orbital signal chain to cleave S2 with the assistance of Nb.BbvCI endonuclease on the electrode surface, resulting in a significant decrease in MB signal. This assay can achieve a LOD as low as 4.57×10^{-6} ng mL^{-1}. Moreover, this aptasensor shows high selectivity, good stability,

and excellent repeatability, providing an effective method for the detection of trace ZEN in corn samples. The Dong group constructed a Zr-MOFs-labeled aptasensor based on Nb.BbvCI-powered DNA walking for PAT detection (Fig. 5B).[116] The aptamer preferentially binds to PAT, inducing the separation of itself from the wDNA and the initiation of the DNA walking machine. The autonomous hybridization of wDNA with the MB@Zr-MOFs/cDNA forms a specific recognition sequence for the Nb.BbvCI enzyme, inducing the cleavage of MB@Zr-MOFs/cDNA by Nb.BbvCI. Eventually, a mass of MB@Zr-MOFs contained in the MB@Zr-MOFs/cDNA is released from the modified electrode surface, resulting in a decrease in the electrical signal. This DNA machine exhibits a LOD of 4.14×10^{-5} ng mL^{-1}, and it can be applied to detect PAT in spiked apple juice and apple wine samples.

Exonucleases are a class of enzymes that can sequentially hydrolyze phosphodiester bonds from the ends of nucleic acid chains to generate single nucleotides. Compared with restriction endonucleases, exonucleases do not require the design of specific recognition sites. Wang *et al.* developed an electrochemical aptasensor based on exonuclease I (Exo I)-assisted target recycling amplification for AFB1 detection (Fig. 5C).[117] Specifically, the ferrocene (Fc)-labeled aptamer forms a hybrid with the MB-labeled complementary DNA of the aptamer to form a duplex structure. Due to the rigid structure of the duplex, Fc molecules are close to the electrode surface and MB molecules are far away, generating a faded external response signal and an enhanced internal reference signal. When AFB1 is present in a sample, the aptamer specifically binds with the target, inducing the detachment of Fc from the electrode surface and a signal-off assay for Fc indicators. Meanwhile, more MB molecules are close to the electrode surface, inducing a signal-on assay for MB indicators. Consequently, the ratiometric electrochemical detection of AFB1 is achieved with the peak current intensity ratio (IMB/IFc) as the signal transducer. In this assay, Exo I is introduced to digest the detached aptamer, and the released AFB1 can subsequently initiate target recycling and signal amplification. This aptasensor exhibits a LOD of 0.032 pg mL^{-1} and can be used to detect AFB1 in actual peanut samples, and achieves results comparable to ELISA. Ren *et al.* designed an electrochemical aptasensor based on an Exo III-powered DNA walker (WDNA) for DON detection (Fig. 5D).[118] In this electrochemical aptasensor, PtPd NPs/PEI-rGO as the substrate material can significantly increase the sensing area, improve the conductivity, and provide the binding sites for nucleic acid strands. The presence of DON can specifically bind to the aptamer, initiating Exo III-assisted cyclic amplification to generate triggers (Tr) (cycle I). Then, the hybridization of Tr with the locking probe (LP) activates the DNA walker (W-DNA) (cycle II). W-DNA runs continuously with the assistance of Exo III, inducing a decrease in the current signal (cycle III). This aptasensor has a LOD of 6.9×10^{-9} mg mL^{-1} and exhibits good stability in real sample analysis. Jin *et al.* constructed a carbon nanocage (CNC)-based fluorescent aptasensor based on T7 Exo-initiated double recycling amplification for AFB1 detection (Fig. 5E).[119] The CNC is introduced as the fluorescence

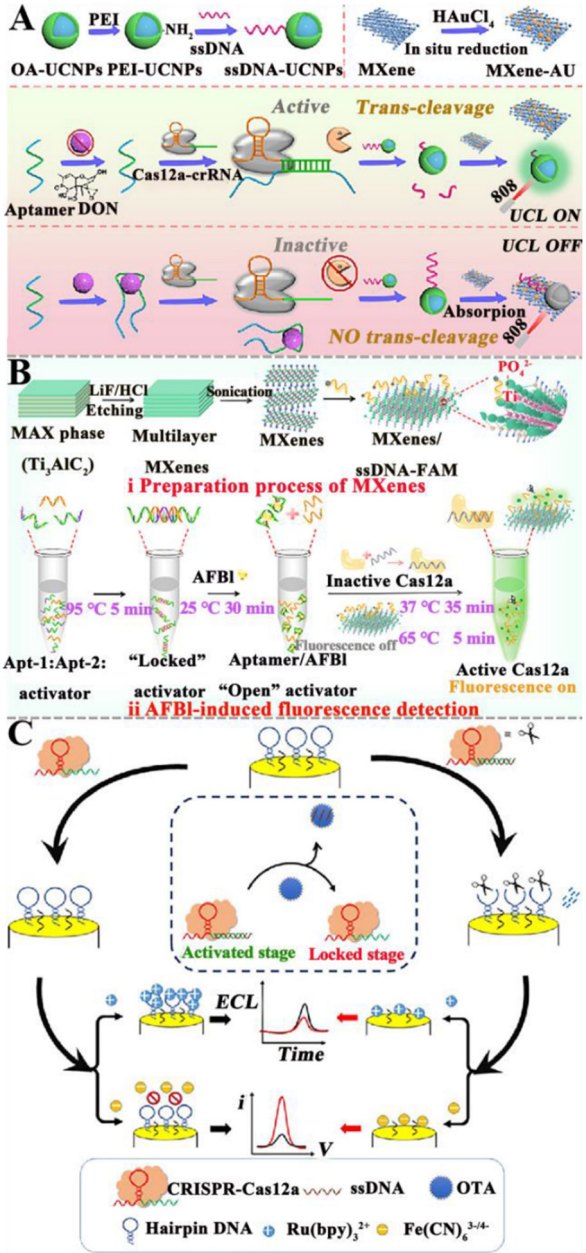

Fig. 6 The construction of aptasensors based on the CRISPR/Cas system for mycotoxin detection. (A) The construction of a CRISPR/Cas12a-modulated LRET aptasensor for the DON assay.[121] (B) The construction of an aptasensor based on the CRISPR/Cas system for the AFB1 assay.[122] (C) The construction of a dual-mode aptasensor based on a target-regulated CRISPR/Cas12a for the OTA assay.[123]

resonance energy transfer (FRET) receptors to quench the fluorophore-labeled DNA probe (FAM-cDNA). In the presence of target AFB1, T7 Exo triggers a double recycling amplification reaction, inducing the digestion of a large number of FAM-cDNAs and the release of FAM fluorophores. This aptasensor can sensitively detect AFB1 with a LOD of 1.4 pg mL^{-1}, and it can be applied in real sample analysis with good recovery results. Notably, even though nucleases can catalyze the cyclic digestion of substrates to achieve the sensitive detection of

target objects, there are some limitations. For example, restriction enzymes need the design of the corresponding cleavage sites, which increases the complexity of the nucleic acid sequence design. In addition, the exonuclease may contain a variety of other catalytic functions and the influence of non-specific catalytic activity should be carefully considered.

3.1.5. CRISPR/Cas system. The clustered regularly interspaced short palindromic repeats (CRISPR) and CRISPR-associated proteins, namely CRISPR/Cas systems, consist of Cas and guide RNA (gRNA).[120] Cas12, Cas13, and Cas14 can cleave both target dsDNA (*cis* cleavage) and non- atopic ssDNA indiscriminately (*trans* cleavage).[124] The *trans* cleavage of ssDNA is efficient (*e.g.*, Cas12a's *trans* cleavage of ssDNA is 1250 times per second) and exhibits excellent signal amplification capability.

3.1.5.1. Integrated with the CRISPR/Cas system directly. The CRISPR/Cas system has shown great potential in nucleic acid biosensing.[72,125] The combination of the CRISPR/Cas system with aptamers can be applied to detect trace mycotoxins. Upon the identification of mycotoxins by aptamers, the cleavage activity of the Cas protein is triggered to achieve signal amplification. Wu *et al.* fabricated a CRISPR/Cas12a-modulated luminescence resonance energy transfer (LRET) aptasensor for the detection of DON (Fig. 6A).[121] The partial hybridization of the DON aptamer with crRNA activates the indiscriminate cleavage activity of Cas12a, resulting in the cleavage of adjacent ssDNA-UCNPs into small fragments. The cleaved ssDNA-UCNPs cannot adsorb on MXene-Au, and the upconversion luminescence (UCL) remains. In the presence of DON, the aptamer binds to DON, leading to the inhibition of the Cas12a activity. As a result, fewer ssDNA-UCNPs are cleaved and more ssDNA-UCNPs can easily adsorb to the MXene-Au surface, leading to the quenching of UCL by LRET. This aptasensor can sensitively detect DON with a LOD of 0.64 ng mL^{-1}, and obtain satisfactory recoveries in corn flour and Tai Lake water. Wei *et al.* developed a fluorescent aptasensor based on CRISPR/Cas12a and MXenes for AFB1 detection (Fig. 6B).[122] In this aptasensor, the ingeniously designed activator is locked by dual-AFB1 aptamers. As a result, the Cas12a and crRNA complexes are inactivated, and the fluorescence of FAM-labeled ssDNA (ssDNA-FAM) is quenched by MXenes. In the presence of AFB1, it binds to the aptamer, inducing the release of the activator. The released activator is complementary to crRNA, activating Cas12a and inducing the cleavage of ssDNA-FAM adsorbed on MXenes and the recovery of fluorescence. This fluorescent aptasensor exhibits a LOD of 0.92 pg mL^{-1} and good assay performance in real peanut samples. Zhu *et al.* constructed a dual-mode aptasensor based on target-regulated CRISPR/Cas12a for OTA detection (Fig. 6C).[123] In the absence of OTA, the crRNA hybridizes with the aptamer to put the CRISPR/Cas12a system in an "active state", inducing the cleavage of hairpin DNA on the electrode and the generation of a weak ECL signal and a high current response. When OTA is present, the aptamer preferentially binds to OTA, resulting in the inhibition of Cas12a activity. The hairpin DNA on the electrode remains intact, resulting in the recovery of the ECL signal and the attenuation of the current signal. This dual-mode aptasensor has high sensitivity and good anti-interference capability, with a wide range of application prospects.

3.1.5.2. NASAT-assisted CRISPR/Cas system. Recently, several NASAT-assisted CRISPR/Cas platforms have been developed for mycotoxin detection. Chen *et al.* constructed a CRISPR/Cas12a-assisted chemiluminescent aptasensor for AFB1 detection (Fig. 7A).[126] This aptasensor takes advantage of the properties of polydopamine (PDA) to self-polymerize and self-assemble into a PDA film through a peroxidation process and subsequently, the biotin-DNA/padlock hybrids can be obtained through the biotin–streptavidin interaction, activating RCA to

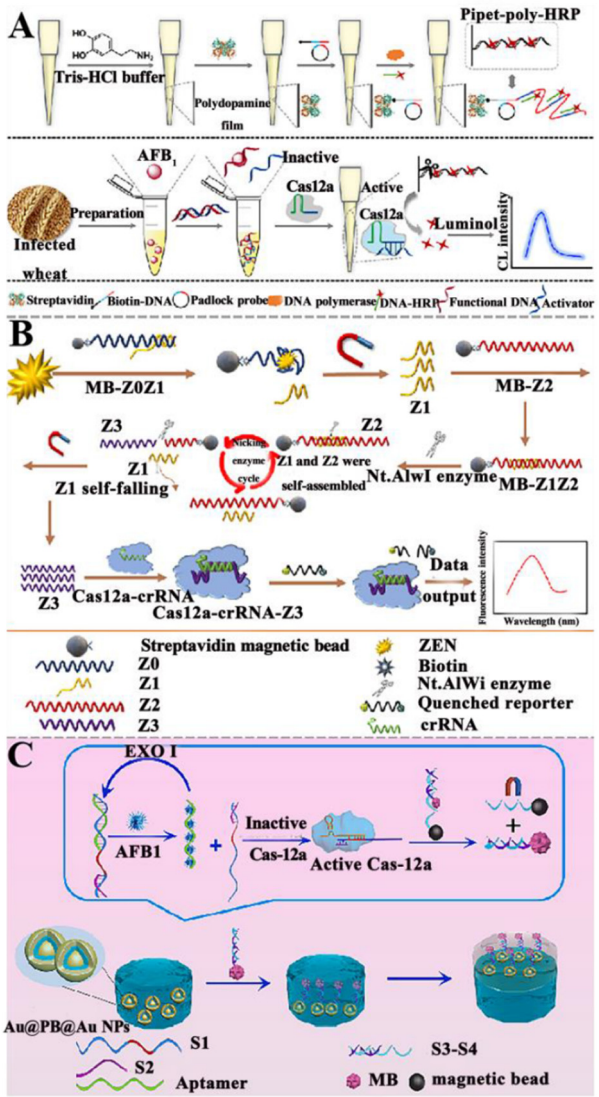

Fig. 7 The construction of aptasensors based on CRISPR/Cas and NASAT for mycotoxin detection. (A) The construction of a CRISPR/Cas12a-assisted chemiluminescent aptasensor for the AFB1 assay.[126] (B) The construction of an aptasensor based on CRISPR/Cas12a and the Nt.A1Wi enzyme for ZEN assay.[127] (C) The construction of a SERS aptasensor based on the CRISPR/Cas system for the AFB1 assay.[128]

produce long linear RCA products with repeated sequences. Finally, a large number of complementary DNA-HRPs are assembled into long, linear RCA products to form the pipette-poly-HRP. In the presence of AFB1, the aptamer preferentially binds to AFB1, resulting in the dissociation of the pre-hybridized aptamer-activator duplex. The released activator hybridizes with the crRNA, initiating the collateral endonuclease activity of Cas12a to degrade the pipet-bound HRP-containing ssDNA linker. As a result, HRPs are released into the solution and quantified by chemiluminescence measurements. This chemiluminescent aptasensor exhibits high sensitivity with a LOD of 5.2 pg mL^{-1}, and it can be applied to measure AFB1 in cereal samples.

Alternatively, Wu *et al.* took advantage of the CRISPR/Cas12a and Nt.A1Wi enzyme to construct an aptasensor for ZEN detection (Fig. 7B).[127] When ZEN is present, it competitively binds to the aptamer Z0, resulting in the release of Z1 into the solution. After magnetic separation, the MB-Z2 probe is added to the supernatant, and two ssDNAs (Z1 & Z2) form a dsDNA. Subsequently, the Nt.AlwI enzyme recognizes the dsDNA and cleaves only the Z2 ssDNA. After enzymatic hydrolysis, Z1 ssDNA and the obtained Z3 ssDNA product are separated from the magnetic beads. The separated Z1 ssDNA can continue to hybridize with Z2 ssDNA, inducing the cleavage of Z2 with the assistance of Nt.AlwI and producing large amounts of ssDNA Z3. The Z3 and CRISPR/Cas12a can form a CRISPR/Cas12a-Z3 complex, activating the trans-cleavage capability of Cas12a to cleave the quenched reporter and induce the recovery of fluorescence. This aptasensor can sensitively detect ZEN with a wide linear range of 1–1000 pg mL^{-1} and a LOD as low as 0.213 pg mL^{-1} and obtain good recovery rates in the corn-oil samples.

Yang *et al.* developed a SERS aptasensor based on CRISPR for the sensitive detection of AFB1 (Fig. 7C).[128] DNA strands modified with –COOH (S4) are coated on the surface of Fe_3O_4 NPs, and the Fe_3O_4 NPs are modified with $-NH_2$ through peptide bonds to form the magnetic core–shell structure nanoparticles. Prussian blue (PB) is embedded in the core–shell nanoparticles, and then the ≡CN of the PB molecule and Au form an Au layer outside. When target AFB1 is present, it binds to the aptamer. Under the catalysis of the Exo I enzyme, the target AFB1 is recycled, and the released S1–S2 structure can activate cas12a, inducing the separation of double strands with beacon molecules from the magnetic beads. The double-strand DNA (dsDNA) with beacon molecules can conjugate with Au@PB@Au NPs through the Au–S bond, and then self-assemble at the water–oil interface. Cyclohexane is used as an oil-phase solvent to form a water–oil two-phase interface, facilitating the formation of nanoparticle film at the interface and the generation of a distinct SERS signal. This SERS aptasensor can sensitively measure AFB1 with a LOD of 3.55 pg mL^{-1}, and lead to a good recovery rate in milk and soy sauce. Although the CRISPR/Cas-based aptasensor has the advantages of being fast, with low cost and high practicality, its accuracy and sensitivity

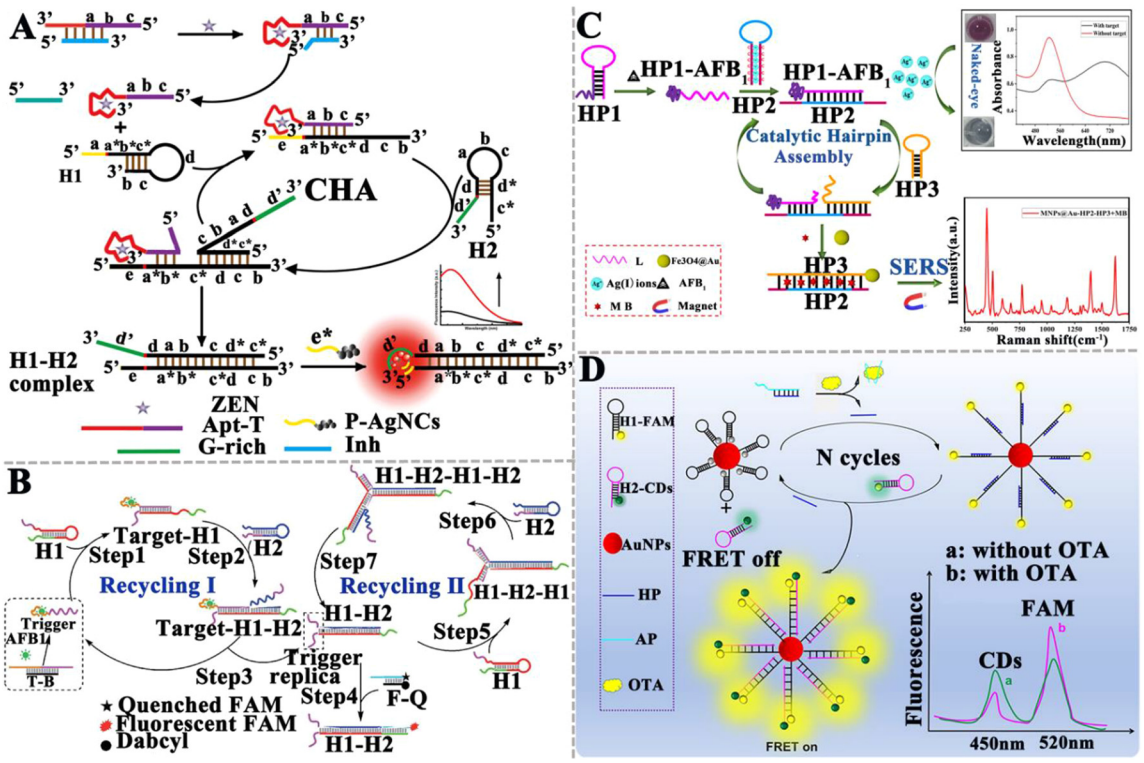

Fig. 8 The construction of CHA-based aptasensors for mycotoxin detection. (A) The construction of a CHA-based fluorometric aptasensor for ZEN assay.[129] (B) The construction of a CHA-based aptasensor for the AFB1 assay.[130] (C) The construction of a dual-mode aptasensor for the AFB1 assay.[131] (D) The construction of a CHA-based FRET aptasensor for the ratiometric detection of OTA.[132]

still need to be systematically verified in real sample analyses. It is, therefore, necessary to use enzyme-linked immunosorbent or other mature methods to confirm the accuracy of results.

3.2. Enzyme-free nucleic acid amplification-based aptasensors

In comparison with enzyme-assisted nucleic acid amplification, enzyme-free amplification does not involve any protein enzymes (*e.g.*, nucleases, ligases, and polymerases) to facilitate nucleic acid signal amplification,[72] efficiently eliminating the issues of protein enzyme instability, high cost, and susceptibility to experimental conditions (*e.g.*, ion concentration, temperature, and pH value).[125] Enzyme-free amplification can be easily carried out in complex biological samples through programmable cascade hybridization reactions.[72] The reported enzyme-free nucleic acid amplification for mycotoxin detection includes catalytic hairpin assembly (CHA), hybridization chain reaction (HCR), DNA tweezers, and DNAzymes.

3.2.1. Catalytic hairpin assembly (CHA). Target-induced CHA uses nucleic acid hybridization as a power to assemble DNA hairpin probes.[125] Gao *et al.* developed a CHA-based fluorometric aptasensor for ZEN detection (Fig. 8A).[129] In the presence of ZEN, the aptamer-triggered sequence (Apt-T) binds to ZEN, inducing the release of the inhibit sequence (Inh) from the Apt-T/Inh duplex. The free Apt-T can open hairpins H1 and H2 to generate an H1–H2 duplex structure. The released Apt-T can subsequently trigger the next round of CHA between H1 and H2. Eventually, the hybridization between H1 and the silver nanocluster (AgNC) probe causes the G-rich sequence to be in close proximity to the non-luminous AgNCs, lighting up the AgNCs and generating an enhanced fluorescence signal. This fluorometric aptasensor achieved a linear range from 1.3 pg mL^{-1} to 100 ng mL^{-1} and a LOD of 0.32 pg mL^{-1}, and it can accurately measure ZEN in maize and beer. Yang *et al.* constructed a CHA-based aptasensor for AFB1 detection (Fig. 8B).[130] In this aptasensor, two split trigger DNA sequences are integrated into two hairpin-assisted probes H1 and H2, respectively, to block the trigger DNA. In the presence of AFB1, the aptamer recognizes and binds to AFB1, exploring the trigger DNA sequence to form a helix DNA H1–H2 complex. The helix DNA H1–H2 complex dissociates the dsDNA probe (F-Q) and restores the fluorescence signal. Meanwhile, two split trigger DNA sequences can form a replica of trigger DNA, triggering new CHA and generating an enhanced fluorescence signal. This aptasensor enables the rapid and sensitive detection of AFB1 with a LOD of 0.13 ng mL^{-1} and exhibits good assay performance in beer and infant rice cereal samples.

Li *et al.* developed a surface-enhanced Raman scattering (SERS) dual-mode aptasensor for the homogeneous detection of mycotoxin with the naked eye (Fig. 8C).[131] The specific binding of the aptamer to AFB_1 forms the HP1–AFB_1 complex, and then the HP1–AFB_1 complex hybridizes with Ag^+-labeled

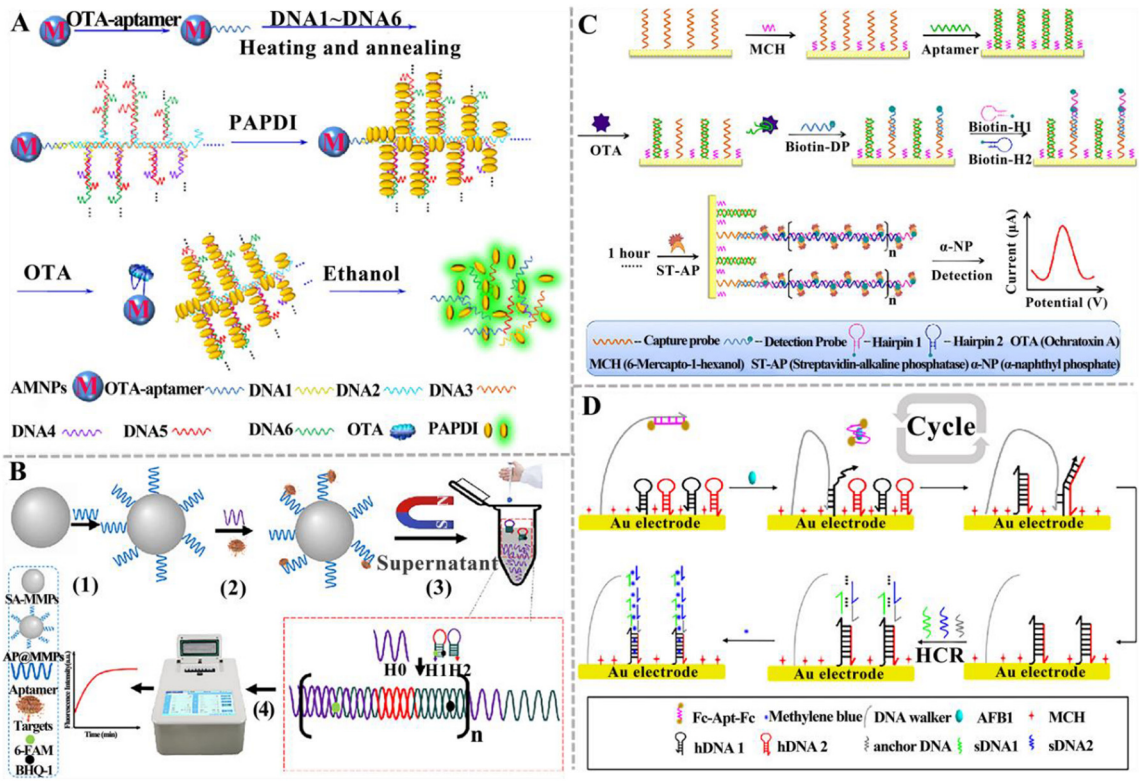

Fig. 9 The construction of HCR-based aptasensors for mycotoxin detection. (A) The construction of an HCR-based aptasensor for the OTA assay.[133] (B) The construction of an HCR-based fluorescent aptasensor for the simultaneous detection of the T-2 toxin and ZEN.[134] (C) The construction of an HCR-based electrochemical aptasensor for the OTA assay.[135] (D) The construction of an HCR-based electrochemical aptasensor for the ratiometric detection of AFB1.[136]

hairpin DNA (HP2), inducing the release of Ag^+ and initiating an enzyme-free CHA reaction to form the dsDNA (HP2–HP3), accompanied by the release of the HP1–AFB_1 complex. The released HP1–AFB_1 complexes can be subsequently recognized by HP2 and HP3, triggering the cascade recycling amplification and resulting in the accumulation of abundant free Ag^+ and the HP2–HP3 duplex. As a result, MB is embedded into the HP2–HP3 duplex and acts as a Raman tag to generate a strong SERS signal with the aid of Fe_3O_4@Au. Meanwhile, the free Ag^+ induces the aggregation of gold nanoparticles (AuNPs) and consequently, a visually distinguishable color change from red to black-blue. The SERS intensity and visualization signals are linearly correlated with the AFB1 concentration in the range of 0.0156–31.2 ng mL^{-1} and 0.61-39 ng mL^{-1}, respectively. The LOD was determined to be 1.6 pg mL^{-1} for the SERS assay and 152 pg mL^{-1} for the colorimetric assay. The He group constructed a CHA-based Förster resonance energy transfer (FRET) aptasensor for the ratiometric detection of OTA (Fig. 8D).[132] In the presence of OTA, the aptamer specifically interacts with OTA, inducing the release of helper DNA (HP). Subsequently, HP opens the hairpin structure of FAM-labeled hairpin DNA 1 (H1-FAM) modified on the AuNP surface. CHA between H1-FAM and hairpin H2 that is labeled with carbon quantum dots (H2-CDs) induces the release of HP, which initiates the next cycle reaction and the occurrence of FRET between CD and FAM. Taking advantage of the measurement of the FCDs/FFAM ratio, this aptasensor can sensitively detect OTA with a wide linear range from 5.0 pg mL^{-1} to 3.0 ng mL^{-1} and a LOD of 1.5 pg mL^{-1}, and it has been successfully applied in the detection of OTA in rice.

3.2.2. Hybridization chain reaction (HCR). The HCR is an amplification technology that uses nucleic acid hybridization as a driving force to achieve a large assembly between DNA hairpin probes.[125] The HCR is an enzyme-free isothermal amplification technique based on a chain reaction of recognition and hybridization events between a pair of complementary and kinetically trapped hairpins.[137] HCR is a simple, enzyme-free, and kinetically controlled signal amplification approach with high amplification efficiency,[137,138] and it has been widely applied in the construction of aptasensors for mycotoxin detection.[133,135,139,140] Li *et al.* developed an aptasensor based on HCR and fluorescent perylene probe (PAPDI)/DNA composites for OTA detection (Fig. 9A).[133] They designed and synthesized PAPDI as the fluorescent probe. HCR induced the aggregation of PAPDI and consequently, the quenching of fluorescence. When OTA is present, it binds to the aptamer, inducing the release of the PAPDI/DNA concatamers from the amino-modified magnetic nanoparticles. After magnetic separation, the supernatant is diluted with ethanol to disaggregate the PAPDI/DNA concatamers. The concentration of OTA can be determined by measuring the fluorescence of disaggregated PAPDI monomers. This aptasensor can detect OTA with a LOD of 0.10 pM. Han *et al.* developed a fluorescent aptasensor based on HCR for the simultaneous detection of T-2 toxin and ZEN (Fig. 9B).[134] Streptavidin-modified magnetic spheres interact with biotin-modified aptamers, resulting in the formation of aptamer-functionalized magnetic microspheres (MMPs) that can specifically capture targets T-2 and ZEN. When the targets and H0 (the initiator chain of HCR) coexist, they competitively bind to aptamers on the magnetic sphere, and the free H0 can subsequently hybridize with 6-FAM and BHQ-1-modified H1 intermediates and H2 to trigger HCR amplification. The measured LOD is 0.1 pg mL^{-1} for T-2 and 1.2 pg mL^{-1} for ZEN. This fluorescent aptasensor can selectively detect T-2 and ZEN in the spiked corn and oat flour samples.

Qiu *et al.* constructed an electrochemical aptasensor based on HCR to detect OTA (Fig. 9C).[135] In this assay, a capture probe is immobilized on the electrode and then hybridizes with the OTA aptamer (Apt) to form an Apt/DNA duplex. The presence of OTA induces the formation of an Apt-OTA complex and the dissociation of Apt from the electrode. Upon the addition of the detection probe and two hairpin-helper DNAs, HCR was activated to extend dsDNA polymers on the electrode surface. Finally, a streptavidin-alkaline phosphatase (ST-AP) conjugate was added to bind biotin-modified hairpin DNA. AP can hydrolyze a synthetic enzyme substrate (α-naphthyl phosphate) to produce a differential pulse voltammetry (DPV) current. The DPV current was enhanced with the increasing concentration of OTA. This electrochemical aptasensor can detect OTA with a LOD of 2 pg mL^{-1}, and it can be applied to measure OTA in cereal samples. You and co-workers established an electrochemical aptasensor for the ratiometric detection of AFB1 (Fig. 9D).[136] This assay involves a dual-amplification by coupling HCR with a DNA walker. The DNA walker strand, hairpin DNA 1 (hDNA1), and hairpin DNA 2 (hDNA2) were initially assembled on the surface of the gold electrode (AuE) *via* Au–S bonds. The DNA walker strand was blocked by the AFB1 aptamer that was modified with ferrocene (Fc). When AFB1 is present, it specifically binds to Fc-Apt-Fc, resulting in the release of the Fc-labelled aptamer (Fc-Apt-Fc) and the decrease in current (I_{Fc}). Subsequently, the DNA walker strand hybridizes with hDNA1 through a toehold-mediated strand exchange, and then hDNA2 hybridizes with hDNA1 to form the dsDNA, initiating a cyclic reaction with the assistance of the DNA walker strand. Meanwhile, the free hDNA1 hybridizes with hDNA2 to form the dsDNA, triggering the DNA walker-mediated amplification. The dsDNA subsequently hybridizes with the anchored DNA to activate HCR between sDNA1 and sDNA2, generating a longer dsDNA that can adsorb MB. AFB1 can be accurately quantified by measuring the current ratio of MB (IMB) and Fc (IFc). The LOD can reach 0.0008 pg mL^{-1}. Consistent results were obtained for this aptasensor and gold-standard HPLC-MS/MS method for peanut sample analysis. Notably, even though HCR-based aptasensors have been widely used for mycotoxin detection, there are some limitations. Because HCR occurs through the random diffusion of DNA hairpins, the kinetics and efficiency are relatively low. The smooth opening of the hairpin structure heavily relies on the sequence design.

3.2.3. DNA tweezer. DNA tweezers are dynamic DNA nanodevices that can reversibly switch their state between open and closed by adding DNA fuel strands.[141,142] DNA tweezers have

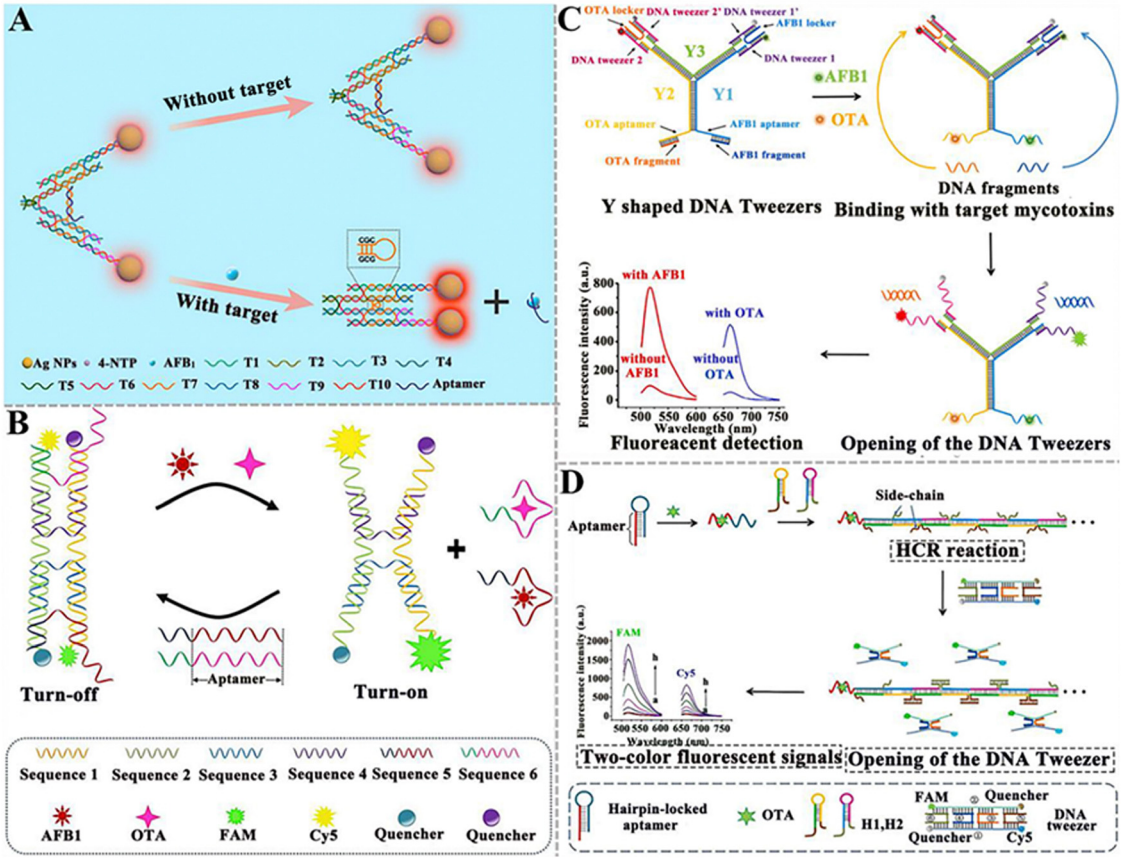

Fig. 10 The construction of DNA tweezer-based aptasensors for mycotoxin detection. (A) The construction of a programmable DNA tweezer-actuated SERS aptasensor for the AFB1 assay.[142] (B) The construction of a dual DNA tweezer-based aptasensor for the simultaneous detection of AFB1 and OTA.[143] (C) The construction of a versatile Y-shaped DNA nanostructure-based aptasensor for the detection of AFB1 and OTA.[144] (D) The construction of a two-color aptasensor based on HCR and DNA tweezers for the OTA assay.[145]

unique superiority in sensor design due to their simple structure and straightforward response mechanism.[143] A series of DNA tweezer-based aptasensors have been constructed for mycotoxin detection. The Han group developed a programmable DNA tweezer-actuated SERS aptasensor for AFB1 detection (Fig. 10A).[142] In this aptasensor, two DNA and 4-nitrothiophenol (4-NTP)-modified AgNPs are linked to the arms of the DNA tweezer, and then the AFB1 aptamer is incorporated into the DNA tweezer by partial DNA hybridization. AgNPs are modified at two arms of the DNA tweezer *via* Ag–S bonds to obtain DNA tweezer-actuated SERS probes. Two AgNPs are separated at the open state, generating a negligible SERS signal. When AFB1 is present, the aptamer binds to it, inducing the release of the aptamer from the DNA tweezer and the formation of a closed state. As a result, two AgNPs are at a closer distance, generating a significantly enhanced SERS signal. This SERS aptasensor can detect AFB1 with a LOD of 5.07 fg mL^{-1}. The Yang group developed a dual DNA tweezer-based nanomachine for the simultaneous detection of AFB1 and OTA (Fig. 10B).[143] The dual DNA tweezers are formed at both ends of the DNA nanomachine and they share two long-arm sequences. The fluorophore and quencher are modified at the ends of two arms of each DNA tweezer, respectively. The two arms of DNA tweezers are locked closely by the aptamer strands of mycotoxins, resulting in the quenching of fluorescence. In the presence of AFB1 and OTA, the aptamer strands bind to their corresponding targets, respectively, resulting in the opening of the DNA tweezers and the recovery of fluorescence. This method is very sensitive with a LOD of 3.5×10^{-2} ppb for AFB1 and 0.1 ppb for OTA. Yang *et al.* developed a versatile Y-shaped DNA nanostructure-based aptasensor for the detection of AFB1 and OTA (Fig. 10C).[144] In this assay, Y-shaped duplex DNA arms are formed with two DNA tweezers at the two ends, resulting in the closing of the DNA tweezers and the quenching of the fluorescence. The tails at the third end contain aptamers of AFB1 and OTA, respectively, which can bind to the corresponding mycotoxins and induce the release of two DNA fragments. The released DNA fragments can open the DNA tweezers, inducing the separation of the fluorophore from the quenching agent and the recovery of fluorescence. AFB1 and OTA can be quantitatively analyzed by measuring the fluorescence intensities of FAM and Cy5, respectively. This assay can be completed in one step within 40 min. Moreover, it can be applied to detect AFB1 and OTA in real food samples. The Yang group developed a two-color aptasensor based on HCR and DNA tweezers for OTA detection (Fig. 10D).[145] OTA can specifically bind to the hairpin

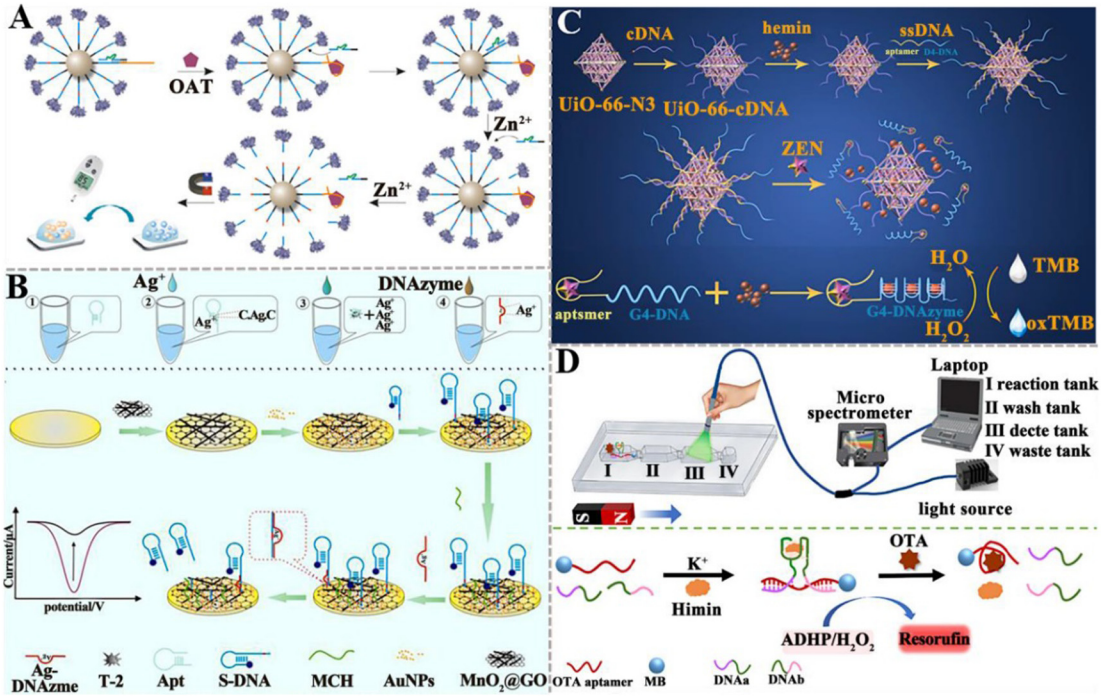

Fig. 11 The construction of DNAzyme-based aptasensors for mycotoxin detection. (A) The construction of an aptasensor based on PGM and DNAzyme for OTA assay.[151] (B) The construction of an electrochemical aptasensor based on Ag^+-dependent DNAzyme-assisted signal amplification for the T-2 toxin assay.[152] (C) The construction of a colorimetric aptasensor based on a stimuli-responsive MOF nano-container and DNAzyme for the ZEN assay.[153] (D) The construction of a portable fluorescent/colorimetric aptasensor based on the G-quadruplex DNAzyme for the rapid and dual-mode detection of OTA.[154]

lock aptamer, inducing the opening of the hairpin structure and triggering the HCR reaction to form a long duplex structure. The formed duplex structure brings the two tails of the hairpin close together, forming two kinds of entire side-chain DNAs on either side. The obtained side-chain DNAs are complementary to the two locker sequences on the two sides of the DNA tweezers, respectively, resulting in the release of two locker sequences and the opening of the DNA tweezers and consequently, the recovery of two-color fluorescence signals. The two-color fluorescence intensities can be used to quantitatively analyze the OTA concentration, with a LOD of 0.006 ppb for FAM and 0.014 ppb for Cy5. Notably, the formation of the DNA tweezer structure usually requires the hybridization and complementation of several single-stranded DNA strands, which may be affected by various experimental conditions. Since the yield of DNA tweezers directly affects the signal amplification efficiency, reducing the complexity of the DNA tweezer as much as possible and increasing its yield can greatly improve the signal amplification efficiency.

3.2.4. DNAzyme. DNAzymes refer to artificially selected DNA fragments with a special stable structure, and they are characterized by high catalytic efficiency, good thermal stability, ease of modification, and low cost.[146] The introduction of DNAzymes into aptasensors significantly improves their analytical performance.[147–150] Specifically, some DNAzymes with peroxidase-mimicking activities can replace the expensive proteases under strict conditions. Lu *et al.* developed an aptasensor based on a personal glucose meter (PGM) and DNAzyme for OTA detection (Fig. 11A).[151] In this aptasensor, biotin-labeled OTA aptamer probes are coupled to streptavidin-labeled substrate chains on magnetic beads (MBs). The DNAzyme hybridizes with the aptamer probe to block the cleavage activity of substrates. In the presence of OTA, the aptamer specifically binds to OTA, inducing the release of the DNAzyme strand and the hybridization between the DNAzyme strand and the substrate strand and consequently, the initiation of the signal amplification reaction of hydrolysis and the cleavage of the substrate chain with the assistance of Zn^{2+}. Since the substrate chain is labeled with invertase (an enzyme that catalyzes the hydrolysis of sucrose to glucose), the OTA signal can be simply converted into a glucose measurement. This DNAzyme-based aptasensor can sensitively detect OTA with a LOD of as low as 0.88 pg mL^{-1} using a PGM as a reader. This assay is selective and easy to perform without the involvement of either expensive instruments or professional operators. It can be a useful supplement to the standard HPLC-MS method, especially for rapid analysis in the field. He *et al.* constructed an electrochemical aptasensor for the sensitive detection of T-2 toxin based on Ag^+-dependent DNAzyme-assisted signal amplification and gold nanoparticles/graphene oxide @ manganese dioxide (AuNPs/MnO_2@GO) nanocomposites (Fig. 11B).[152] In this electrochemical aptasensor, the secondary structure of the T-2 aptamer is altered *via* the Ag^+-mediated coordination of C–Ag^+–C base pairs. When T-2 toxin is present, its interaction

Table 3 A summary of NASAT-based aptasensors for mycotoxin assay

Amplification strategy	Signal model	Target	Linear range (ng mL^{-1})	LOD (ng mL^{-1})	Real sample	Ref.
RT-qPCR	Fluorescence	AFM1	1.0×10^{-4}–1.0	3×10^{-5}	Rice, milk	76
RT-qPCR	Fluorescence	AFB1	3.12×10^{-5}–3.12	3×10^{-5}	Soy sauce, milk, yellow wine, and peanut butter	77
RT-qPCR	qPCR	OTA	0.039–1000	0.009	Beer	75
RCA	Electrochemical	OTA	1.0×10^{-4}–5.0	6.5×10^{-5}	Wine	103
RCA	Colorimetric	AFB1	1.0×10^{-5}–1.2×10^{-4}	1.4×10^{-5}	Rice, peanut oil	104
RCT	Fluorescence	OTA	0.0001–0.5	1.94×10^{-5}	Milk	105
SDA	Electrochemical	ZEN	1.0×10^{-3}–0.15	1.8×10^{-4}	Corn	110
SDA	Fluorescence	AFB1, ZEN	1.0×10^{-3}–10, 1.0×10^{-2}–100	9.33×10^{-4}; 1.07×10^{-3}	Cornmeal	111
SDA	Fluorescence	PAT	0.001–100	4.2×10^{-5}	Apple and grape juices	112
SDA	Fluorescence	AFM1, OTA	1.968×10^{-2}–0.1968 2.498×10^{-2}–4.03	0.01779; 0.01898	Milk	113
Nicking endonuclease-assisted amplification	Electrochemical	ZEN	1.0×10^{-4}–1.0×10^{3}	4.57×10^{-6}	Corn	115
Nicking endonuclease-assisted amplification	Electrochemical	PAT	5.0×10^{-6}–5.0×10^{-1}	4.14×10^{-5}	Apple juice, apple wine	116
ExoI-assisted amplification	Electrochemical	AFB1	1.0×10^{-4}–1.0	3.2×10^{-5}	Peanut	117
ExoIII-assisted amplification	Electrochemical	DON	1.0×10^{-2}–1.0×10^{2}	6.9×10^{-3}	Maize flour	118
T7 Exo-assisted amplification	Fluorescence	AFB1	0.01–500.0	1.4×10^{-3}	Instant grains, peanut, corn flour, Chinese herb (QC-522B-1)	119
CRISPR/Cas	Luminescence	DON	1.0–500.0	0.64	Corn flour, Tai Lake water	121
CRISPR/Cas	Fluorescence	AFB1	0.001–80.0	9.2×10^{-4}	Peanut	122
CRISPR/Cas	Electrochemiluminescent, Electrochemical	OTA	1.0×10^{-3}–5.0, 1.0×10^{-3}–5.0	2.9×10^{-4}; 3.7×10^{-4}	Morinda officinalis	123
CRISPR/Cas & Nt.AlwI	Fluorescence	ZEN	1.0×10^{-3}–1.0	2.13×10^{-4}	Corn oil	127
CRISPR-Cas12a & RCA	Chemiluminescence	AFB1	0.05–100.0	5.2×10^{-3}	Wheat	126
CRISPR/Cas & Exo I	SERS	AFB1	0.001–1.5	3.55×10^{-3}	Milk, soy sauce	128
CHA	Fluorescence	ZEN	1.3×10^{-3}–100	3.2×10^{-4}	Maize, beer	129
CHA	Fluorescence	AFB1	0.30–15.0	0.13	Beer, infant rice cereal	130
CHA	SERS, colorimetric	AFB1	0.0156–31.2; 0.61–39.0	1.6×10^{-3}; 0.152	Wheat	131
CHA	Fluorescence	OTA	5.0×10^{-3}–3.0	1.5×10^{-3}	Rice	132
HCR	Fluorescence	OTA	4.038×10^{-4}–8.076×10^{-3}	4.038×10^{-5}	Corn	133
HCR	Electrochemical	OTA	0.005–100.0	2.0×10^{-3}	Corn, wheat	135
HCR	Electrochemical	AFB1	3.0×10^{-6}–3×10^{-3}	8.8×10^{-7}	Peanut	136
HCR	Fluorescence	T-2, ZEN	0.001–10.0, 0.01–100.0	1.0×10^{-4}; 1.2×10^{-3}	Corn, oat flour	134
DNA Tweezer	SERS	AFB1	1.0×10^{-5}–1.0	5.07×10^{-6}	Maize	142
DNA Tweezer	Fluorescence	AFB1, OTA	8.0×10^{-2}–10.0, 0.5–50.0	3.5×10^{-2}; 0.1	Corn, peanut, coffee, olive oil, peanut oil	143
HCR & DNA Tweezer	Dual-fluorescence	OTA	0.02–0.8	0.006 for FAM; 0.014 for Cy5	Peanut, corn, sesame, coffee beans, peanut oil, Soybean oil	145
DNA Tweezer	Fluorescence	AFB1, OTA	0.5–200.0, 4.0–300.0	0.1; 2.0	Sesame, olive oil	144
DNAzyme	personal glucose meter	OTA	1.0×10^{-3}–300.0	8.8×10^{-4}	Wine	151
DNAzyme	Electrochemical	T-2	2.0×10^{-6}–20.0	1.07×10^{-7}	Milk	152
DNAzyme	Colorimetric	ZEN	0.01–100.0	3.6×10^{-4}	Maize, wheat	153
DNAzyme	Fluorescent, Colorimetric	OTA	5.0–100.0, 0.05–10.0	0.011; 0.008	Wheat	154

with the Apt will change the secondary structure of Apt, releasing silver ions. The free Ag^+ can activate a specific RNA-cleaving DNAzyme to cleave the S-DNA immobilized on the surface of AuNPs/MnO2@GO-modified electrode, resulting in the introduction of 6-mercapto-1-hexanol (MCH) to block non-specific binding sites. Subsequently, the DNAzyme repeatedly binds and cleaves MB-modified S-DNA with the aid of Ag^+, leading to a decrease in the electrochemical signal. The LOD can reach 0.107 fg mL^{-1}. This electrochemical aptasensor can accurately measure the T-2 toxin in beer.

DNAzymes mimic peroxidase is an excellent alternative to natural peroxidase and has recently been explored for mycotoxin detection. Wang *et al.* developed a colorimetric aptasensor based on a stimuli-responsive metal–organic framework (MOF) nano-container and DNAzyme for ZEN detection (Fig. 11C).[153] In this aptasensor, an azide-functionalized MOF (UiO-66-N3) functions as a nano-container to entrap hemin after being conjugated with DBCO-functionalized cDNA. The bio-gate composed of a DNA duplex acts as a gatekeeper to control the release. When ZEN is present, it competes for the binding sites of aptamers with cDNA, inducing the opening of hybrid duplexes and the unlocking of pores. The presence of ZEN induces the concentration-dependent release of hemin and ssDNA (containing trimeric CatG4) into the supernatant. Subsequently, hemin is embedded into the secondary structure of trimer CatG4, inducing its conversion to a trivalent G4-DNAzyme that possesses higher catalytical activity than hemin itself. Upon the addition of TMB, the liquid emits a strong colorimetric signal. This colorimetric aptasensor can detect ZEN with a LOD of 0.36 pg mL^{-1}. Chen *et al.* constructed a portable fluorescent/colorimetric aptasensor based on G-quadruplex DNAzyme for the rapid and dual-mode detection of OTA (Fig. 11D).[154] The OTA aptamers and MBs can self-assemble with two segments of DNA and hemin to form a G-quadruplex DNAzyme structure that can catalyse the oxidation of Amplex Red (ADHP) by H_2O_2, inducing the change in solution color to red and the generation of a strong fluorescence. When OTA is present, it specifically binds to aptamers, inducing the decomposition of the DNA enzyme structure and decreasing its catalytic activity. Under optimal conditions, this aptasensor can measure OTA with a LOD of 0.011 μg kg^{-1} for the fluorescence mode and 0.008 μg kg^{-1} for the colorimetric mode.

4. Conclusions and perspectives

The perennial hot topic of food safety and contamination has attracted more and more attention around the world due to its direct impact on human health and social harmony. The main assurance is to continuously develop rapid and sensitive detection methods for food pollutants in the entire food supply chain, from farm to fork/plate. However, conventional methods for mycotoxin assay are not suitable for rapid and sensitive assays. Alternatively, a variety of aptasensors have been constructed for mycotoxin detection in recent years. To overcome the limitation of low signals generated by mycotoxins, nucleic acid signal amplification technology (NASAT) has been introduced into the aptasensors to significantly improve the sensitivity and facilitate the detection of low-abundance mycotoxins. Herein, we have provided a comprehensive review of the recent advances in NASAT-based aptasensors for mycotoxin assay, and summarized the principles, features, and applications of NASAT-based aptasensors. The NASAT is divided into enzyme-assisted and enzyme-free nucleic acid amplification approaches. The working principles and practical applications of NASAT-based aptasensors for mycotoxin detection are summarized in Table 3.

Despite great progress made in the development of NASAT-based aptasensors for mycotoxin assay, several challenges remain to be solved. (1) Few mycotoxin aptamers have been reported so far. In addition, the aptamer matching degree is low in complex matrix environments, and some invalid sequences may affect the stability of aptamer binding and increase the synthesis cost.[155] It is essential to improve the screening procedure by combining ''positive SELEX'' with ''negative SELEX'', which can efficiently eliminate the influence of the matrix and obtain highly specific aptamer sequences.[52] (2) At present, the detection of mycotoxins is challenged by the coexistence of multiple targets.[156,157] The discovery of new aptamer molecules and an increase in target coverage is highly required, which facilitates the construction of efficient aptasensors for high-throughput and the simultaneous detection of multiple mycotoxins. (3) The reported aptasensors are limited to a single mode that suffers from false positives. The development of dual-mode aptasensors that combine different output modes (*e.g.*, fluorometric, colorimetric, and electrochemical measurements) greatly improves the detection accuracy.[136,154] (4) Due to the trace levels of mycotoxins in foods, NASATs are often involved in the construction of aptasensors for the ultrasensitive detection of mycotoxins.[69] Notably, some amplification approaches have the limitations of non-specific amplification and high cost. The discovery of low-cost and low-background signal amplification strategies can significantly improve the detection sensitivity. (5) To overcome the inherent amplification bias and non-specific amplification in NASAT, the introduction of nanomaterials (*e.g.*, metal nanoparticles, carbon nanotubes, GO, and UCNPs) into amplification reactions may minimize the amplification bias and eliminate the non-specific amplification.[119,132,152,158,159] Compared with the nanosensors used directly for mycotoxin detection, the aptasensors based on nanomaterials and NASAT possess improved sensitivity, facilitating the ultra-sensitive monitoring of mycotoxins in complex food substrates from farm to table. (6) The NASAT-based aptasensors for mycotoxin detection reported above are largely limited to laboratory assays. Given the extensive and real-time food contamination occurrences, the rapid, accurate, modest, and reliable onsite detection system is imperative, particularly in the vast rural regions where resources are scarce. Portable instruments (*e.g.*, side-flow analysis, microfluidic devices, and smartphone-based point-of-care testing (POCT)) have been applied in simple,

rapid, and low-cost field inspections. However, the reported side-flow analysis, microfluidic devices, and smartphone-based POCT for mycotoxin detection usually rely on antibodies that are expensive to produce, and the use of animals for this purpose may raise ethical concerns.[158,160–163] The introduction of NASAT-based aptasensors into the side-flow analysis and microfluidic system may significantly improve the sensitivity, overcoming the issue of low field detection sensitivity.[164–168] In addition, the use of smartphones to analyze the output signal not only satisfies the portability of the field detection equipment but also ensures the reliability and stability of the result analysis as compared with the naked eye. Above all, the prospects of NASAT-based aptasensors include the following: (1) going from ultra-sensitive detection in the laboratory to rapid and sensitive detection in the field; (2) making the detection process more intelligent and automated; (3) high-throughput analysis of mycotoxins from single-factor analysis to multi-target detection. We believe that with the development of nanomaterials, microfluidics, and new technologies, NASAT-based aptasensors will play more and more important roles in food safety.

Author contributions

Dandan Zhang: writing the original draft, reviewing, and editing. Ting Luo: reviewing and editing. Xiangyue Cai: reviewing and editing. Ning-ning Zhao: reviewing and editing. Chun-yang Zhang: reviewing, editing, and supervision.

Conflicts of interest

There are no conflicts to declare.

Acknowledgements

This work was supported by Teacher Development Research Start-up Fund of Chengdu University of Technology (10912-KYQD2020-08414).

Notes and references

1 W. Zhu, L. Li, Z. Zhou, X. Yang, N. Hao, Y. Guo and K. Wang, *Food Chem.*, 2020, **319**, 126544.
2 S. Marin, A. J. Ramos, G. Cano-Sancho and V. Sanchis, *Food Chem. Toxicol.*, 2013, **60**, 218–237.
3 Q. Jiang, J. Wu, K. Yao, Y. Yin, M. M. Gong, C. Yang and F. Lin, *ACS Sens.*, 2019, **4**, 3072–3079.
4 Y. Yang, G. Li, D. Wu, J. Liu, X. Li, P. Luo, N. Hu, H. Wang and Y. Wu, *Trends Food Sci. Technol.*, 2020, **96**, 233–252.
5 Q. Zhou and D. Tang, *TrAC-Trend Anal. Chem.*, 2020, **124**, 115814.
6 S. Brase, A. Encinas, J. Keck and C. F. Nising, *Chem. Rev.*, 2009, **109**, 3903–3990.
7 W. P. Liew and S. Mohd-Redzwan, *Front. Cell. Infect. Microbiol.*, 2018, **8**, 60.
8 J. Wen, P. Mu and Y. Deng, *Toxicol. Res.*, 2016, **5**, 377–387.
9 M. Jia, X. Liao, L. Fang, B. Jia, M. Liu, D. Li, L. Zhou and W. Kong, *TrAC-Trend Anal. Chem.*, 2021, **136**, 116193.
10 Z. Gong, Y. Huang, X. Hu, J. Zhang, Q. Chen and H. Chen, *Biosensors*, 2023, **13**, 140–173.
11 A. L. Capriotti, G. Caruso, C. Cavaliere, P. Foglia, R. Samperi and A. Lagana, *Mass Spectrom. Rev.*, 2012, **31**, 466–503.
12 S. Agriopoulou, E. Stamatelopoulou and T. Varzakas, *Foods*, 2020, **9**, 518–540.
13 A. Mousavi Khaneghah, A. Farhadi, A. Nematollahi, Y. Vasseghian and Y. Fakhri, *Trends Food Sci. Technol.*, 2020, **102**, 193–202.
14 X. Tang, J. Zuo, C. Yang, J. Jiang, Q. Zhang, J. Ping and P. Li, *TrAC-Trend Anal. Chem.*, 2023, **165**, 117144.
15 Y. Liu and F. Wu, *Environ. Health Perspect.*, 2010, **118**, 818–824.
16 L. Xu, Z. Zhang, Q. Zhang and P. Li, *Toxins*, 2016, **8**, 239–254.
17 Z. Xue, Y. Zhang, W. Yu, J. Zhang, J. Wang, F. Wan, Y. Kim, Y. Liu and X. Kou, *Anal. Chim. Acta*, 2019, **1069**, 1–27.
18 A. Gallo, G. Giuberti, J. C. Frisvad, T. Bertuzzi and K. F. Nielsen, *Toxins*, 2015, **7**, 3057–3111.
19 R. Li, Y. Wen, F. Wang and P. He, *J. Anim. Sci. Biotechnol.*, 2021, **12**, 108.
20 L. Zhang, X. W. Dou, C. Zhang, A. F. Logrieco and M. H. Yang, *Toxins*, 2018, **10**, 65–103.
21 A. Alshannaq and J. H. Yu, *Int. J. Environ. Res. Public Health*, 2017, **14**, 632–651.
22 T. I. Ekwomadu, T. A. Dada, S. A. Akinola, N. Nleya and M. Mwanza, *Separations*, 2021, **8**, 143–154.
23 J. He, B. Zhang, H. Zhang, L. L. Hao, T. Z. Ma, J. Wang and S. Y. Han, *J. Food Sci.*, 2019, **84**, 2688–2697.
24 M. Solfrizzo, L. Gambacorta, R. Bibi, M. Ciriaci, A. Paoloni and I. Pecorelli, *J. AOAC Int.*, 2018, **101**, 647–657.
25 Y. Fan, J. Li, K. Amin, H. Yu, H. Yang, Z. Guo and J. Liu, *Food Res. Int.*, 2023, **170**, 113022.
26 M. Majdinasab, S. Ben Aissa and J. L. Marty, *Toxins*, 2020, **13**, 13–47.
27 M. E. E. Alahi and S. C. Mukhopadhyay, *Sensors*, 2017, **17**, 1885–1904.
28 S.-C. Pei, W.-J. Lee, G.-P. Zhang, X.-F. Hu, S. A. Eremin and L.-J. Zhang, *Food Control*, 2013, **31**, 65–70.
29 H. Peng, Y. Chang, R. C. Baker and G. Zhang, *Food Addit. Contam.: Part A*, 2020, **37**, 496–506.
30 X. Liu, G. Ying, X. Liao, C. Sun, F. Wei, X. Xing, L. Shi, Y. Sun, W. Kong and L. Zhou, *Anal. Chem.*, 2019, **91**, 1194–1202.
31 C. Sun, X. Liao, P. Huang, G. Shan, X. Ma, L. Fu, L. Zhou and W. Kong, *Food Chem.*, 2020, **315**, 126289.
32 L. Qin, J. Y. Jiang, L. Zhang, X. W. Dou, Z. Ouyang, L. Wan and M. H. Yang, *Mycology*, 2020, **11**, 126–146.
33 S. D. Jayasena, *Clin. Chem.*, 1999, **45**, 1628–1650.
34 N. Zhang, B. Liu, X. Cui, Y. Li, J. Tang, H. Wang, D. Zhang and Z. Li, *Talanta*, 2021, **223**, 121729.
35 S. Ni, Z. Zhuo, Y. Pan, Y. Yu, F. Li, J. Liu, L. Wang, X. Wu, D. Li, Y. Wan, L. Zhang, Z. Yang, B. T. Zhang, A. Lu and G. Zhang, *ACS Appl. Mater. Interfaces*, 2021, **13**, 9500–9519.
36 G. Zon, *Anal. Biochem.*, 2022, **644**, 113894.
37 J. Chen, X. Zhang, S. Cai, D. Wu, M. Chen, S. Wang and J. Zhang, *Biosens. Bioelectron.*, 2014, **57**, 226–231.
38 F. Costantini, C. Sberna, G. Petrucci, M. Reverberi, F. Domenici, C. Fanelli, C. Manetti, G. de Cesare, M. DeRosa, A. Nascetti and D. Caputo, *Sens. Actuators, B*, 2016, **230**, 31–39.
39 S. Perrier, Z. Zhu, E. Fiore, C. Ravelet, V. Guieu and E. Peyrin, *Anal. Chem.*, 2014, **86**, 4233–4240.
40 A. Ruscito, M. Smith, D. N. Goudreau and M. C. DeRosa, *J. AOAC Int.*, 2016, **99**, 865–877.
41 C. Wang, J. Qian, K. Wang, K. Wang, Q. Liu, X. Dong, C. Wang and X. Huang, *Biosens. Bioelectron.*, 2015, **68**, 783–790.
42 Q. Zhao, Q. Lv and H. Wang, *Anal. Chem.*, 2014, **86**, 1238–1245.
43 S. Wu, N. Duan, X. Ma, Y. Xia, H. Wang, Z. Wang and Q. Zhang, *Anal. Chem.*, 2012, **84**, 6263–6270.
44 B. Wang, Y. Chen, Y. Wu, B. Weng, Y. Liu, Z. Lu, C. M. Li and C. Yu, *Biosens. Bioelectron.*, 2016, **78**, 23–30.
45 Y. Seok, J. Y. Byun, W. B. Shim and M. G. Kim, *Anal. Chim. Acta*, 2015, **886**, 182–187.
46 W. B. Shim, M. J. Kim, H. Mun and M. G. Kim, *Biosens. Bioelectron.*, 2014, **62**, 288–294.
47 A. Shrivastava and R. K. Sharma, *Toxin Rev.*, 2021, **41**, 618–638.
48 X. Chen, Y. Huang, N. Duan, S. Wu, Y. Xia, X. Ma, C. Zhu, Y. Jiang and Z. Wang, *J. Agric. Food Chem.*, 2014, **62**, 10368–10374.
49 M. McKeague, R. Velu, K. Hill, V. Bardoczy, T. Meszaros and M. C. DeRosa, *Toxins*, 2014, **6**, 2435–2452.

50 X. Wang, X. Gao, J. He, X. Hu, Y. Li, X. Li, L. Fan and H. Z. Yu, *Analyst*, 2019, **144**, 3826–3835.
51 X. Wei, P. Ma, K. Imran Mahmood, Y. Zhang and Z. Wang, *J. Agric. Food Chem.*, 2023, **71**, 7546–7556.
52 J. A. Cruz-Aguado and G. Penner, *J. Agric. Food Chem.*, 2008, **56**, 10456–10461.
53 M. McKeague, C. R. Bradley, A. De Girolamo, A. Visconti, J. D. Miller and M. C. Derosa, *Int. J. Mol. Sci.*, 2010, **11**, 4864–4881.
54 J. W. Park, R. Tatavarty, D. W. Kim, H. T. Jung and M. B. Gu, *Chem. Commun.*, 2012, **48**, 2071–2073.
55 B. R. Rushing and M. I. Selim, *Food Chem. Toxicol.*, 2019, **124**, 81–100.
56 Y. Tao, S. Xie, F. Xu, A. Liu, Y. Wang, D. Chen, Y. Pan, L. Huang, D. Peng, X. Wang and Z. Yuan, *Food Chem. Toxicol.*, 2018, **112**, 320–331.
57 D. Liu, L. Ge, Q. Wang, J. Su, X. Chen, C. Wang and K. Huang, *Environ. Int.*, 2020, **143**, 105949.
58 T. Kuiper-Goodman, P. M. Scott and H. Watanabe, *Regul. Toxicol. Pharmacol.*, 1987, **7**, 253–306.
59 A. V. Nathanail, E. Varga, J. Meng-Reiterer, C. Bueschl, H. Michlmayr, A. Malachova, P. Fruhmann, M. Jestoi, K. Peltonen, G. Adam, M. Lemmens, R. Schuhmacher and F. Berthiller, *J. Agric. Food Chem.*, 2015, **63**, 7862–7872.
60 G. J. A. Speijers, M. A. M. Franken and F. X. R. V. Leeuwen, *Food Chem. Toxicol.*, 1988, **26**, 23–30.
61 D.-l Li, X. Zhang, Y. Ma, Y. Deng, R. Hu and Y. Yang, *Anal. Methods*, 2018, **10**, 3273–3279.
62 H. Guo, P. Ma, K. Li, S. Zhang, Y. Zhang, H. Guo and Z. Wang, *Sens. Actuators, B*, 2022, **358**, 131484.
63 C. Zhu, D. Liu, Y. Li, S. Ma, M. Wang and T. You, *Biosens. Bioelectron.*, 2021, **174**, 112654.
64 D. Yang, Y. Hui, Y. Liu, W. Wang, C. He, A. Zhao, L. Wei and B. Wang, *Food Chem.*, 2024, **433**, 137362.
65 S. Xiang, J. Li, F. Wang, H. Yang, Y. Jiang, P. Zhang, R. Cai and W. Tan, *Anal. Chem.*, 2023, **95**, 15125–15132.
66 Z. Wu, E. Xu, M. F. J. Chughtai, Z. Jin and J. Irudayaraj, *Food Chem.*, 2017, **230**, 673–680.
67 W. Yu, X. Lin, N. Duan, Z. Wang and S. Wu, *Anal. Chim. Acta*, 2023, **1244**, 340846.
68 X. Zhao, H. Shen, B. Huo, Y. Wang and Z. Gao, *Biosens. Bioelectron.*, 2022, **211**, 114383.
69 J. Zhou, T. Y. Wang, Z. Lan, H. J. Yang, X. J. Ye, R. Min, Z. H. Wang, Q. Huang, J. Cao, Y. E. Gao, W. L. Wang, X. L. Sun and Y. Zhang, *Food Res. Int.*, 2023, **173**, 113286.
70 Y. Zhao, F. Chen, Q. Li, L. Wang and C. Fan, *Chem. Rev.*, 2015, **115**, 12491–12545.
71 F. Ma, C. C. Li and C. Y. Zhang, *Chem. Commun.*, 2021, **57**, 13415–13428.
72 W.-j Liu, X. Zhang, F. Ma and C.-y Zhang, *TrAC-Trend Anal. Chem.*, 2023, **160**, 116998.
73 M. Joshi and J. D. Deshpande., *Int. J. Biomed. Res.*, 2011, **5**, 81–97.
74 N. Arnheim and H. Erlich, *Annu. Rev. Biochem.*, 1992, **61**, 131–156.
75 H. Modh, T. Scheper and J. G. Walter, *Eng. Life Sci.*, 2017, **17**, 923–930.
76 X. Guo, F. Wen, N. Zheng, S. Li, M. L. Fauconnier and J. Wang, *Anal. Bioanal. Chem.*, 2016, **408**, 5577–5584.
77 J. Sun, X. Ning, L. Cui, W. Qin, W. Wang and S. He, *Food Chem.*, 2024, **432**, 137240.
78 S. Bi, S. Yue and S. Zhang, *Chem. Soc. Rev.*, 2017, **46**, 4281–4298.
79 N. Zhang, J. Li, B. Liu, D. Zhang, C. Zhang, Y. Guo, X. Chu, W. Wang, H. Wang, X. Yan and Z. Li, *Talanta*, 2022, **236**, 122866.
80 W. Zhao, M. M. Ali, M. A. Brook and Y. Li, *Angew. Chem., Int. Ed.*, 2008, **47**, 6330–6337.
81 M. M. Ali, F. Li, Z. Zhang, K. Zhang, D. K. Kang, J. A. Ankrum, X. C. Le and W. Zhao, *Chem. Soc. Rev.*, 2014, **43**, 3324–3341.
82 W. Zhao, C. H. Cui, S. Bose, D. Guo, C. Shen, W. P. Wong, K. Halvorsen, O. C. Farokhzad, G. S. Teo, J. A. Phillips, D. M. Dorfman, R. Karnik and J. M. Karp, *Proc. Natl. Acad. Sci. U. S. A.*, 2012, **109**, 19626–19631.
83 Z. Zhang, M. M. Ali, M. A. Eckert, D. K. Kang, Y. Y. Chen, L. S. Sender, D. A. Fruman and W. Zhao, *Biomaterials*, 2013, **34**, 9728–9735.
84 L. Tang, Y. Liu, M. M. Ali, D. K. Kang, W. Zhao and J. Li, *Anal. Chem.*, 2012, **84**, 4711–4717.
85 Z. Cheglakov, Y. Weizmann, B. Basnar and I. Willner, *Org. Biomol. Chem.*, 2007, **5**, 223–225.
86 M. M. Ali and Y. Li, *Angew. Chem., Int. Ed.*, 2009, **48**, 3512–3515.
87 H. Dong, C. Wang, Y. Xiong, H. Lu, H. Ju and X. Zhang, *Biosens. Bioelectron.*, 2013, **41**, 348–353.
88 F. Dahl, J. Banér, M. Gullberg, M. Mendel-Hartvig, U. Landegren and M. Nilsson, *Proc. Natl. Acad. Sci. U. S. A.*, 2004, **101**, 4548–4553.
89 W. Zhao, Y. Gao, S. A. Kandadai, M. A. Brook and Y. Li, *Angew. Chem., Int. Ed.*, 2006, **45**, 2409–2413.
90 S. Beyer, P. Nickels and F. C. Simmel, *Nano Lett.*, 2005, **5**, 719–722.
91 H. Su, R. Yuan, Y. Chai, L. Mao and Y. Zhuo, *Biosens. Bioelectron.*, 2011, **26**, 4601–4604.
92 L. Linck, E. Reiß, F. Bier and U. Resch-Genger, *Anal. Methods*, 2012, **4**, 1215–1220.
93 A. Berr and I. Schubert, *Plant J.*, 2006, **45**, 857–862.
94 M. McKeague, A. De Girolamo, S. Valenzano, M. Pascale, A. Ruscito, R. Velu, N. R. Frost, K. Hill, M. Smith, E. M. McConnell and M. C. DeRosa, *Anal. Chem.*, 2015, **87**, 8608–8612.
95 W.-B. Shim, H. Mun, H.-A. Joung, J. A. Ofori, D.-H. Chung and M.-G. Kim, *Food Control*, 2014, **36**, 30–35.
96 X. Ma, W. Wang, X. Chen, Y. Xia, S. Wu, N. Duan and Z. Wang, *Eur. Food Res. Technol.*, 2014, **238**, 919–925.
97 K. Setlem, B. Mondal, S. Ramlal and J. Kingston, *Front Microbiol.*, 2016, **7**, 1909.
98 C. Hamula, J. Guthrie, H. Zhang, X. Li and X. Le, *TrAC-Trend Anal. Chem.*, 2006, **25**, 681–691.
99 S. Malhotra, A. K. Pandey, Y. S. Rajput and R. Sharma, *J. Mol. Recognit.*, 2014, **27**, 493–500.
100 X. Chen, Y. Huang, N. Duan, S. Wu, X. Ma, Y. Xia, C. Zhu, Y. Jiang and Z. Wang, *Anal. Bioanal. Chem.*, 2013, **405**, 6573–6581.
101 C. C. Ong, S. Siva Sangu, N. M. Illias, S. Chandra Bose Gopinath and M. S. M. Saheed, *Biosens. Bioelectron.*, 2020, **154**, 112088.
102 S. Wu, N. Duan, W. Zhang, S. Zhao and Z. Wang, *Anal. Biochem.*, 2016, **508**, 58–64.
103 L. Huang, J. Wu, L. Zheng, H. Qian, F. Xue, Y. Wu, D. Pan, S. B. Adeloju and W. Chen, *Anal. Chem.*, 2013, **85**, 10842–10849.
104 W. Wu, S. Xia, M. Zhao, J. Ping, J. M. Lin and Q. Hu, *Anal. Chim. Acta*, 2022, **1220**, 340065.
105 S. Niazi, I. M. Khan, Y. Yu, I. Pasha, Y. Lv, A. Mohsin, B. S. Mushtaq and Z. Wang, *Sens. Actuators, B*, 2020, **315**, 128049.
106 G. T. Walker, M. S. Fraiser, J. L. Schram, M. C. Little, J. G. Nadeau and D. P. Malinowski, *Nucleic Acids Res.*, 1992, **20**, 1691–1696.
107 L. Zhang, H. Jiang, Z. Zhu, J. Liu and B. Li, *Talanta*, 2022, **243**, 123388.
108 C. Yuan, J. Fang, M. L. de la Chapelle, Y. Zhang, X. Zeng, G. Huang, X. Yang and W. Fu, *TrAC-Trend Anal. Chem.*, 2021, **143**, 116401.
109 J. Liu, D. Wu, J. Chen, S. Jia, J. Chen, Y. Wu and G. Li, *Crit. Rev. Food Sci. Nutr.*, 2022, **64**, 2960–2985.
110 X. Zhu, C. Yang, W. Quan, G. Yang, L. Guo and H. Xu, *Anal. Methods*, 2023, **15**, 987–992.
111 Y. Yang, Z. Zhou, Y. Guo, R. Chen, D. Tian, S. Ren, H. Zhou and Z. Gao, *Anal. Chim. Acta*, 2024, **1292**, 342245.
112 M. Zhang, Y. Wang, X. Sun, J. Bai, Y. Peng, B. Ning, Z. Gao and B. Liu, *Anal. Chim. Acta*, 2020, **1106**, 161–167.
113 J. Yin, Y. Liu, S. Wang, J. Deng, X. Lin and J. Gao, *Sens. Actuators, B*, 2018, **256**, 573–579.
114 M. Yan, W. Bai, C. Zhu, Y. Huang, J. Yan and A. Chen, *Biosens. Bioelectron.*, 2016, **77**, 613–623.
115 H. Yan, B. He, R. Zhao, W. Ren, Z. Suo, Y. Xu, Y. Zhang, C. Bai, H. Yan and R. Liu, *J. Hazard. Mater.*, 2022, **438**, 129491.
116 B. He and X. Dong, *Chem. Eng. J.*, 2021, **405**, 126642.
117 H. Cui, K. An, C. Wang, Y. Chen, S. Jia, J. Qian, N. Hao, J. Wei and K. Wang, *Sens. Actuators, B*, 2022, **355**, 131238.
118 K. Wang, B. He, L. Xie, L. Li, J. Yang, R. Liu, M. Wei, H. Jin and W. Ren, *Sens. Actuators, B*, 2021, **349**, 130767.
119 X. Niu, J. Yang, Z. Suo, M. Wei, Y. Liu, B. He and H. Jin, *Microchem. J.*, 2023, **187**, 108418.
120 K. S. Makarova, D. H. Haft, R. Barrangou, S. J. Brouns, E. Charpentier, P. Horvath, S. Moineau, F. J. Mojica, Y. I. Wolf, A. F. Yakunin and J. Van Der Oost, *Nat. Rev. Microbiol.*, 2011, **9**, 467–477.
121 X. Lin, C. Li, X. Meng, W. Yu, N. Duan, Z. Wang and S. Wu, *J. Hazard. Mater.*, 2022, **433**, 128750.

122 Z. Wu, D. W. Sun, H. Pu and Q. Wei, *Talanta*, 2023, **252**, 123773.
123 H. Xu, R. Pan, W. Huang and X. Zhu, *Anal. Methods*, 2023, **15**, 4518–4523.
124 K. S. Makarova, Y. I. Wolf, O. S. Alkhnbashi, F. Costa, S. A. Shah, S. J. Saunders, R. Barrangou, S. J. Brouns, E. Charpentier, D. H. Haft, P. Horvath, S. Moineau, F. J. Mojica, R. M. Terns, M. P. Terns, M. F. White, A. F. Yakunin, R. A. Garrett, J. van der Oost, R. Backofen and E. V. Koonin, *Nat. Rev. Microbiol.*, 2015, **13**, 722–736.
125 Z.-y Wang, P. Li, L. Cui, J.-G. Qiu, B. Jiang and C.-y Zhang, *TrAC-Trend Anal. Chem.*, 2020, **129**, 115959.
126 Z. Wang, L. Wei, S. Ruan and Y. Chen, *J. Agric. Food Chem.*, 2023, **71**, 4417–4425.
127 X. Yao, Q. Yang, Y. Wang, C. Bi, H. Du and W. Wu, *Foods*, 2022, **11**, 487–499.
128 J. Zhang, L. Jiang, H. Li, R. Yuan and X. Yang, *Food Chem.*, 2023, **415**, 135768.
129 N. Yin, S. Yuan, M. Zhang, J. Wang, Y. Li, Y. Peng, J. Bai, B. Ning, J. Liang and Z. Gao, *Microchim. Acta*, 2019, **186**, 765.
130 L. Zhao, J. Mao, L. Hu, S. Zhang and X. Yang, *Anal. Methods*, 2021, **13**, 222–226.
131 Y. Yang, D. Wu, J. Liu, Z. Su, L. Li, Y. Wu and G. Li, *Biosens. Bioelectron.*, 2022, **214**, 114526.
132 H. Zhang, Y. Wang, Y. Lin, W. Chu, Z. Luo, M. Zhao, J. Hu, X. Miao and F. He, *Anal. Bioanal. Chem.*, 2023, **415**, 867–874.
133 B. Wang, Y. Wu, Y. Chen, B. Weng, L. Xu and C. Li, *Biosens. Bioelectron.*, 2016, **81**, 125–130.
134 W. Zhu, G. Ji, R. Chen, Y. Xiang, S. Ji, S. Zhang, Z. Gao, H. Liu, Y. Wang and T. Han, *Talanta*, 2023, **255**, 124249.
135 Y. Qing, X. Li, S. Chen, X. Zhou, M. Luo, X. Xu, C. Li and J. Qiu, *Microchim. Acta*, 2017, **184**, 863–870.
136 F. Jia, D. Liu, N. Dong, Y. Li, S. Meng and T. You, *Biosens. Bioelectron.*, 2021, **182**, 113169.
137 X. Wang, C. Lau, M. Kai and J. Lu, *Analyst*, 2013, **138**, 2691–2697.
138 Y. Lin, J. Wang, F. Luo, L. Guo, B. Qiu and Z. Lin, *Electrochim. Acta*, 2018, **283**, 798–805.
139 J. Tang, Y. Cheng, J. Zheng, J. Li, Y. Sun, S. Peng and Z. Zhu, *Anal. Methods*, 2019, **11**, 5638–5644.
140 Y. Liu, H. Yan, J. Shangguan, X. Yang, M. Wang and W. Liu, *Microchim. Acta*, 2018, **185**, 427.
141 B. Yurke, A. J. Turberfield, A. P. Mills Jr, F. C. Simmel and J. L. Neumann, *Nature*, 2000, **406**, 605–608.
142 J. Li, W. Wang, H. Zhang, Z. Lu, W. Wu, M. Shu and H. Han, *Anal. Chem.*, 2020, **92**, 4900–4907.
143 Z. Xiong, Q. Wang, Y. Xie, N. Li, W. Yun and L. Yang, *Food Chem.*, 2021, **338**, 128122.
144 Q. Ma, D. Nie, X. Sun, Y. Xu, J. He, L. Yang and L. Yang, *Spectrochim. Acta, Part A*, 2022, **281**, 121634.
145 G. Wu, Z. Xiong, S. H. Oh, Y. Ren, Q. Wang and L. Yang, *Food Chem.*, 2021, **356**, 129663.
146 D. Li, S. Song and C. Fan, *Acc. Chem. Res.*, 2010, **43**, 631–641.
147 D. Zhang, F. Ma, J. Leng and C. Y. Zhang, *Chem. Commun.*, 2018, **54**, 13678–13681.
148 Q. Zhang, R. Zhao, C. C. Li, Y. Zhang, C. Tang, X. Luo, F. Ma and C. Y. Zhang, *Anal. Chem.*, 2022, **94**, 13978–13986.
149 N. N. Zhao, Y. Z. Liu, L. Zhang, W. Liu, X. Zou, Q. Xu and C. Y. Zhang, *Anal. Chem.*, 2023, **95**, 12974–12981.
150 L.-j Wang, Q. Liu, F. Ma and C.-y Zhang, *TrAC-Trend Anal. Chem.*, 2023, **167**, 117270.
151 S. Zhang, Y. Luan, M. Xiong, J. Zhang, R. Lake and Y. Lu, *ACS Appl. Mater. Interfaces*, 2021, **13**, 9472–9481.
152 L. Wang, H. Jin, M. Wei, W. Ren, Y. Zhang, L. Jiang, T. Wei and B. He, *Sens. Actuators, B*, 2021, **328**, 129063.
153 Y. Sun, Y. Lv, S. Qi, Y. Zhang and Z. Wang, *Food Chem.*, 2022, **371**, 131145.
154 X. Lin, Y. Fang, Q. Chen, Z. Guo, X. Chen and X. Chen, *Talanta*, 2024, **267**, 125273.
155 E. Schax, M. Lönne, T. Scheper, S. Belkin and J.-G. Walter, *Biotechnol. Bioprocess Eng.*, 2016, **20**, 1016–1025.
156 Z. Han, Z. Tang, K. Jiang, Q. Huang, J. Meng, D. Nie and Z. Zhao, *Biosens. Bioelectron.*, 2020, **150**, 111894.
157 G. Ge, T. Wang, Z. Liu, X. Liu, T. Li, Y. Chen, J. Fan, E. Bukye, X. Huang and L. Song, *Talanta*, 2023, **265**, 124908.
158 K.-Y. Xing, S. Shan, D.-F. Liu and W.-H. Lai, *TrAC-Trend Anal. Chem.*, 2020, **133**, 116087.
159 A. Rhouati, G. Bulbul, U. Latif, A. Hayat, Z. H. Li and J. L. Marty, *Toxins*, 2017, **9**, 349–371.
160 X. Xiang, Q. Ye, Y. Shang, F. Li, B. Zhou, Y. Shao, C. Wang, J. Zhang, L. Xue, M. Chen, Y. Ding and Q. Wu, *Biosens. Bioelectron.*, 2021, **190**, 113394.
161 Z. Suo, X. Niu, M. Wei, H. Jin and B. He, *Anal. Chim. Acta*, 2023, **1246**, 340888.
162 L. Shi, Y. Li, C. Jia, J. Shan, S. Wang, S. Liu, J. Sun, D. Zhang, Y. Ji and J. Wang, *Trends Food Sci. Technol.*, 2023, **138**, 100–115.
163 E. M. Khalaf, H. Sanaan Jabbar, R. Mireya Romero-Parra, G. Raheem Lateef Al-Awsi, H. Setia Budi, A. S. Altamimi, M. Abdulfadhil Gatea, K. T. Falih, K. Singh and K. A. Alkhuzai, *Microchem. J.*, 2023, **190**, 108692.
164 C. Wu, Y. Yue, B. Huang, H. Ji, L. Wu and H. Huang, *Talanta*, 2024, **269**, 125414.
165 Y. Lan, B. He, C. S. Tan and D. Ming, *Biosensors*, 2022, **12**, 477–488.
166 X. Xiang, M. Song, X. Xu, J. Lu, Y. Chen, S. Chen, Y. He and Y. Shang, *Anal. Chem.*, 2023, **95**, 7993–8001.
167 A. Jaisankar, S. Krishnan and L. Rangasamy, *Anal. Biochem.*, 2022, **655**, 114874.
168 W. K. Abdelbasset, S. V. Savina, D. Mavaluru, R. A. Shichiyakh, D. O. Bokov and Y. F. Mustafa, *Talanta*, 2023, **252**, 123769.

